PNWD-3344
WTP-RPT-083 Rev. 0

Thermodynamic Data Development for Modeling Sr/TRU Separations: Sr-EDTA, Sr-HEDTA, and Mn-Gluconate Complexation

A. R. Felmy
M. J. Mason
O. Qafoku

September 2003

Prepared for Bechtel National, Inc.
under Contract 24590-101-TSA-W000-00004

LEGAL NOTICE

This report was prepared by Battelle Memorial Institute (Battelle) as an account of sponsored research activities. Neither Client nor Battelle nor any person acting on behalf of either:

MAKES ANY WARRANTY OR REPRESENTATION, EXPRESS OR IMPLIED, with respect to the accuracy, completeness, or usefulness of the information contained in this report, or that the use of any information, apparatus, process, or composition disclosed in this report may not infringe privately owned rights; or

Assumes any liabilities with respect to the use of, or for damages resulting from the use of, any information, apparatus, process, or composition disclosed in this report.

Reference herein to any specific commercial product, process, or service by trade name, trademark, manufacturer, or otherwise, does not necessarily constitute or imply its endorsement, recommendation, or favoring by Battelle. The views and opinions of authors expressed herein do not necessarily state or reflect those of Battelle.

Thermodynamic Data Development for Modeling Sr/TRU Separations: Sr-EDTA, Sr-HEDTA, and Mn-Gluconate Complexation

A. R. Felmy
M. J. Mason
O. Qafoku

September 2003

Test Specification: NA
Test Plan: NA
Test Exceptions: None
R&T Focus Area: Pretreatment
Testing Scoping Statement: B-37

Battelle—Pacific Northwest Division
Richland, Washington 99352

COMPLETENESS OF TESTING

This report provides a summary of all the modeling work done in support of the Sr/TRU removal task. Experimental results from published reports were used to evaluate available thermodynamic data in the open literature and identify areas where additional or improved data was needed. The descriptions provided in this test report are an accurate account of both the conduct of the work and the data analysis. The modeling results and this report have been reviewed and verified.

Approved:

_____ _____

Gordon Beeman, Manager Date
WTP R&T Support Project

Summary

The River Protection Project-Waste Treatment Plant (RPP-WTP) baseline for pretreating Envelope C low-activity waste (LAW) at Hanford includes a precipitation step for removing radioactive strontium (Sr-90) and transuranic (TRU) isotopes before the waste is vitrified. The current design basis for the Sr/TRU removal process is the addition of strontium nitrate (0.075M), for isotopic dilution, and sodium permanganate (0.05M), for TRU removal, at 50°C and 1M additional sodium hydroxide. Section 5 of the *Research and Technology Plan*[(a)] identifies further research needs. One need shown is to determine the mechanism of the Sr/TRU precipitation process (SOW Ref.: Sec. C.6 Std.2(a)(3)(ii)(B) and WBS No.: 1.2.10.01 and .02). Thermodynamic modeling of the Sr/TRU removal process is addressed in Scoping Statement B-37, which is included in Appendix C of the *Research and Technology Plan*. In accordance with Scoping Statement B-37, thermodynamic data were obtained and calculations performed for simple mixtures of organic complexants and simulated supernatant solutions to develop a better understanding of the Sr/TRU removal process.

Objectives

This report summarizes the results of studies conducted to develop improved thermodynamic data for modeling Sr and Mn species to support an understanding of the mechanism of Sr/TRU precipitation from solution. The data development emphasizes three areas: the complexation of Sr by ethylene-diaminetetraacetate (EDTA), the complexation of Sr by N-(2-hydroxyethyl)ethylenedinitrilotriacetic acid (HEDTA), and the complexation of Mn(II, III, and IV) by sodium gluconate. EDTA and HEDTA were chosen for study since they represent the chelates of primary importance in solubilizing Sr in Envelope C wastes. Sodium gluconate was chosen as a model for the type of complexants for tri- and higher valence metal ions. Furthermore, sodium gluconate was used at Hanford in waste processing.

Conduct of Testing

A comprehensive study of the complexation of Sr with EDTA and HEDTA was conducted with the objective of developing accurate aqueous thermodynamic models for predicting the solubility of $SrCO_3$ over a wide range of complexant concentrations, ionic strengths, and temperatures. These efforts are documented in Sections 2.0 and 3.0 of this report. Additional experimental data were provided through funding by the Environmental Management Sciences Program (EMSP), and are available in the open literature.

In the case of Mn and gluconate, the addition of Mn as MnO_4^- (MnVII) can result in the formation of reduced oxidation states of Mn (i.e., II, III, and IV) upon reaction with low molecular weight organics or other reducing species. These reduced oxidation states, especially Mn(IV), have the ability to interact with metal-gluconate complexes present in the waste and displace these metal ions from the complex. This effect is suspected in the case of Fe(III)-gluconate complex in Tank AN-107. Unfortunately, there are no thermodynamic data available for the Mn-gluconate complexes with which to predict these

(a) Bechtel National, Inc. (BNI). 2002. *Research and Technology Plan*. 24590-WTP-PL-RT-01-002, Rev. 1, U.S. Department of Energy, Office of River Protection, Richland, WA.

reactions. Considering these factors, thermodynamic data were developed for the Mn(II, III, and IV) complexes of gluconate based on an analysis of literature data. The validity of these results was at least partly established by modeling the addition of MnO_4^- in Tank AN-107. These results are presented in Section 4.0.

Results and Performance Against Objectives

The objective of this work was to improve the thermodynamic data for modeling the Sr and Mn species to help increase the understanding of the mechanism of Sr/TRU precipitation from Envelope C wastes. Models describing the Na-Sr-OH-CO_3-NO_3-EDTA-H_2O and Na-Sr-OH-CO_3-NO_3-HEDTA-H_2O systems were produced. The models allow the extrapolation of standard-state equilibrium constants for $SrEDTA^{2-}$ and $SrHEDTA^-$ species. In addition, thermodynamic parameters for various Mn-gluconate complexes were calculated and used to determine the impact of permanganate treatment of AN-107 waste, which has the high levels of soluble Fe.

Quality Requirements

Thermodynamic modeling began under funding by British Nuclear Fuels, Ltd. and continued through to support assessment of the reaction mechanisms of Sr/TRU removal by added $Sr(NO_3)_2$ and permanganate. Battelle—Pacific Northwest Division (PNWD) implemented the RPP-WTP quality requirements by performing work in accordance with the quality assurance project plan (QAPjP) approved by the RPP-WTP Quality Assurance (QA) organization. PNWD addressed verification activities by conducting an Independent Technical Review of the final report in accordance with procedure QA-RPP-WTP-604. This review verified that the reported results were traceable, that inferences and conclusions were soundly based, and that the reported work satisfied the goals of Scoping Statement B-37.

Issues

None.

Acknowledgments

This research was supported by the River Protection Project–Waste Treatment Plant (RPP-WTP) under Contract 24590-101-TSA-W000-00004 with Battelle–Pacific Northwest Division, and by the Environmental Management Sciences Program (EMSP) under Project No. 26753, “Chemical Speciation of Strontium, Americium, and Curium in High Level Waste.”

Abbreviations

aq	aqueous
(c)	crystalline
EDTA	ethylenediaminetetraacetate
emf	electromotive force
HEDTA	N-(2-hydroxyethyl) ethylenedinitrilotriacetic acid
I	ionic strength
IC	ion chromatography
ICP-MS	inductively coupled plasma mass spectrometry
IDA	iminodiacetic acid
LAW	low-activity waste
m	molality
M	molarity
NHE	normal hydrogen electrode
NMR	nuclear magnetic resonance
NTA	nitrilotriacetic acid
SCE	standard calomel electrode
TMAC	tetramethylammonium chloride
TRU	transuranic
V	volts
XRD	X-ray diffraction
β_{ij}	general second virial coefficient
C_{ijk}	general third virial coefficient
θ	second virial coefficient for anion-anion interactions
ψ	third virial coefficient for anion-anion-cation interactions

Contents

Figures

Tables

1.0 Introduction

This report summarizes work performed by Battelle—Pacific Northwest Division (PNWD) in support of the River Protection Project-Waste Treatment Plant (RPP-WTP) at Hanford. Two tanks at Hanford (Tanks AN-102 and AN-107) that are scheduled for processing in the waste treatment plant contain high concentrations of organic complexing agents (designated as Envelope C[(a)] wastes). The high complexant concentration results in significant concentrations of radioactive species in the liquid, supernatant, fraction of the waste destined for vitrification as low-activity waste (LAW). A wide range of organic complexants were initially used in waste processing, and many fragments and degradation products from aging during storage are now present in the waste. Some known and suspected compounds include ethylenediaminetetraacetate (EDTA), N-(2-hydroxyethyl) ethylenedinitrilotriacetic acid (HEDTA), nitrilotriacetic acid (NTA), iminodiacetic acid (IDA), citric acid, glycolic acid, sodium gluconate, sodium oxalate, and sodium formate. A Sr/TRU removal process was developed for treatment of the Envelope C wastes. The Sr-90 removal process consists of isotopic dilution by nonradioactive $Sr(NO_3)_2$ addition and precipitation of $SrCO_3$. The TRU removal process involves addition of permanganate; stepwise manganese reduction, Mn(VII) to Mn(VI) to Mn(IV); precipitation of MnO_2; and concomitant TRU precipitation. Entrained solids and Sr/TRU precipitate are to be removed via crossflow filtration.

Felmy (2000) reported the initial results for modeling the [Sr] and $SrCO_3$ precipitation with data from treatment of diluted AN-107 waste. The results supported that the primary mechanism for Sr-90 removal is isotopic dilution by added nonradioactive $Sr(NO_3)_2$ and $SrCO_3$ precipitation. The addition of permanganate increases the Sr-90 decontamination, likely a result of oxidation of the chelating agents and precipitation of additional $SrCO_3$. The Sr-90 decontamination factors increased significantly with time. However, this increased Sr-90 decontamination was not a result of increased isotopic exchange or ligand oxidation, but, rather, continued precipitation, i.e., reduction of total soluble Sr concentration. Isotopic exchange was found to be complete 18 min after reagent addition was complete (Hallen et al. 2002). Therefore, in addition to isotopic dilution, $SrCO_3$ precipitation is important in decontamination of Sr-90. Additional thermodynamic data were needed to understand the Sr-90 removal process. The needed data included [Sr] as a function of the sodium concentration, carbonate concentration, complexant concentration, temperature, and time.

The early modeling efforts of Felmy (2000) were not consistent with the experimental results for TRU removal by the permanganate treatment. In particular, actual waste tests showed precipitation of Mn solids and approximately 99% of the soluble Fe on treatment, whereas the model did not predict Fe precipitation. Sodium gluconate is suspected of complexing several metal ions, including Fe and possibly Am/Cm. The addition of Mn as MnO_4^- during Sr/TRU separations can influence the behavior of these metal ions, since Mn as MnO_4^- (oxidation state VI) is rapidly reduced to lower oxidation states. These lower oxidation states, especially Mn(IV), Mn(III), and possibly Mn(II), have the potential of interacting with gluconate and altering the efficiency of the separation process. Unfortunately, thermodynamic data are unavailable for these Mn-gluconate complexes. Such data are needed to understand the influence of Mn addition on the formation of metal-gluconate complexes.

(a) Envelope designations are explained in DOE (2000).

The objective of the work reported here was to assemble and analyze all of the available thermodynamic data with respect to the Sr/TRU removal process. This work focused specifically on the complexation of added Sr and Mn.

The results from all of the modeling work in support of the Sr/TRU removal process are summarized in this report. The Sr-EDTA modeling work is described in Section 2.0; Sr-HEDTA work in Section 3.0; and Mn-gluconate work in Section 4.0. The major conclusions and recommendations are given in Section 5.0. The appendix includes the analyses of the potentiometer data for Mn-gluconate complexes.

1.1 Quality Assurance Requirements

PNWD implements the RPP-WTP quality requirements by performing work in accordance with the PNWD Waste Treatment Plant Support Project quality assurance project plan (QAPjP) approved by the RPP-WTP Quality Assurance (QA) organization. This work was performed to the quality requirements of NQA-1-1989 Part I, Basic and Supplementary Requirements, and NQA-2a-1990, Subpart 2.7. These quality requirements are implemented through PNWD's *Waste Treatment Plant Support Project (WTPSP) Quality Assurance Requirements and Description Manual*. The analytical requirements are implemented through PNWD's *Conducting Analytical Work in Support of Regulatory Programs*.

Experiments that are not method-specific were performed in accordance with PNWD's procedures QA-RPP-WTP-1101 "Scientific Investigations" and QA-RPP-WTP-1201 "Calibration Control System," assuring that sufficient data were taken with properly calibrated measuring and test equipment (M&TE) to obtain quality results.

BNI's QAPjP, 24590-QA-0001, is not applicable since the work was not performed in support of environmental/regulatory testing, and the data should not be used as such.

PNWD addressed internal verification and validation activities by conducting an Independent Technical Review of the final data report in accordance with PNWD's procedure QA-RPP-WTP-604. This review verified that the reported results were traceable, that inferences and conclusions were soundly based, and the reported work satisfied the Test Plan objectives. This review procedure is part of the *WTPSP Quality Assurance Requirements and Description Manual*.

2.0 An Aqueous Thermodynamic Model for the Complexation of Strontium with EDTA Valid to High Ionic Strength

The development of an aqueous thermodynamic model for Sr and EDTA is discussed in this section (Felmy and Mason 2003). The model accurately describes the effects of Na^+ complexation, ionic strength (I), carbonate concentration, and temperature on the complexation of Sr^{2+} by EDTA under basic conditions. The model is developed from the analysis of literature data on apparent equilibrium constants, enthalpies, and heat capacities, as well as on an extensive set of solubility data on $SrCO_3$(c) in the presence of EDTA obtained as part of this study. The solubility data for $SrCO_3$(c) were obtained in solutions ranging in Na_2CO_3 concentration from 0.01m to 1.8m, in $NaNO_3$ concentration from 0 to 5m, and at temperatures extending to 75°C. The final aqueous thermodynamic model is based on the equations of Pitzer and requires the inclusion of a $NaEDTA^{3-}$ species. An accurate model for the ionic strength dependence of the ion-interaction coefficients for the $SrEDTA^{2-}$ and $NaEDTA^{3-}$ aqueous species allows the extrapolation of standard-state equilibrium constants for these species, which are significantly different from the 0.1m reference-state values available in the literature. The final model is tested by application to chemical systems containing competing metal ions (i.e., Ca^{2+}) to further verify the proposed model and indicate the applicability of the model parameters to chemical systems containing other divalent metal-EDTA complexes.

2.1 Background Literature

The organic complexation of Sr has been studied by many researchers, and for various applications. In addition to the specific issue of organic complexation of Sr by the organic chelators in high-level nuclear wastes, such strong organic chelating agents are important in a variety of chemical engineering applications. For example, the importance of EDTA is so prevalent that in the recent compilation of stability constants for metal ion complexes (Martell and Smith 1995) there are over 160 association constants for EDTA-metal ions with 70 different elements or different oxidation states. However, of the over 160 complexes with critically reviewed and recommended stability constants, the thermodynamic data for only four complexes ($CaEDTA^{2-}$, $ZnEDTA^{2-}$, $HfEDTA^{2+}$ and $ZrEDTA^{2+}$) have recommended values reported for zero ionic strength. The vast majority of the stability constants are reported for the 0.1M reference state or other ionic strengths. Interestingly, there is a very large variation in the stability constants for these complexes in the extrapolation to zero ionic strength (Table 2.1).

Table 2.1. Standard-State (I=0.0M) and Reference-State (I =0.1M) Stability Constants for Metal-EDTA Complexes (Martell and Smith 1995)

Complex	Log K I=0.0M	Log K I=0.1M	Difference
$CaEDTA^{2-}$	12.42	10.65, 10.97	+1.45 to +1.77
$ZnEDTA^{2-}$	18.0	16.5	+1.5
$HfEDTA^{2+}$	33.7	29.5	+4.2
$ZrEDTA^{2+}$	32.8	29.4	+3.4

The effects of ionic strength, or in our specific case, interactions of the major cation in nuclear waste (Na^+), with the organic chelates must therefore be resolved before accurate aqueous thermodynamic models can be developed for calculating the concentrations of the metal-organic chelate complexes in these solutions. Fortunately, the thermodynamics of alkali metal association with EDTA and other chelates has been the objective of intensive experimental studies, including studies to high ionic strength (Nelson 1955; Palaty 1963; James and Noggle 1969; Vasil'ev and Belonogova 1976; Daniele et al. 1985; Hovey et al. 1988; Chen and Reid 1993; Mizera et al. 1999). Unfortunately, although the stability constants of Sr-EDTA complexes have been examined numerous times (see the compilations of Anderegg 1975 and Martell and Smith 1995), little data exist on the high ionic strength dependence of the stability constants for these species, and only one study extends to the high carbonate conditions typical of tank processing applications (Felmy and Mason 1998) at 25°C.

With these factors in mind, the specific objective of this study was to develop accurate aqueous thermodynamic models for the Na^+-$EDTA^{4-}$ ion interactions and $SrEDTA^{2-}$ species interactions that are valid over a range of temperatures (25°C to 75°C) and extend to high ionic strength (~9m). To achieve this objective, we tabulated a wide range of literature data on the ionic strength and temperature dependence of the formation constants for $NaEDTA^{3-}$ and $SrEDTA^{2-}$ species, extended the experimental studies on $SrCO_3$(c) solubility of Felmy and Mason (1998) to 50°C and 75°C, and extended the range of ionic strength to as high as 9m with the addition of $NaNO_3$. $SrCO_3$(c) was selected for study, since it is likely to be the solubility-limiting phase in environmental (vadose zone) applications near leaking waste tanks and in waste tank processing applications designed to remove Sr-90.

2.2 Experimental Procedures

The experimental studies on the solubility of $SrCO_3$(c) at room temperature (22-23°C) were conducted in the same general manner as previously described by Felmy and Mason (1998). Briefly, all solubility studies at room temperature were conducted in a controlled atmosphere chamber filled with nitrogen gas to prevent contact between solutions and atmospheric CO_2. For these studies, 2.5 g of reagent-grade $SrCO_3$(c) were added to 50-ml polypropylene centrifuge tubes. Stock solutions of reagent-grade NaOH, $NaNO_3$, Na_2CO_3, and $Na_4EDTA{\cdot}2H_2O$ were prepared, and aliquots of these solutions were combined to give a final solution volume of approximately 30 ml. NaOH concentrations were maintained at 0.1M to ensure all of the added Na_2CO_3 was present as the carbonate ion and to prevent the formation of any protonated EDTA [i.e., $H(EDTA)^{3-}$ species]. Na_2CO_3 concentrations ranged from initial values of 0.01M to approximately 1.8M. The final carbonate concentrations increased significantly at the lower initial added carbonate values, owing to the dissolution of the $SrCO_3$ precipitate upon the addition of EDTA. Suspensions were placed in an orbital shaker and shaken, then sampled at various times to determine, or establish, equilibrium conditions. Sampling consisted of pH measurements, at NaOH concentrations lower than 0.1M, followed by centrifugation at 2000 g for 7 to 10 min. Aliquots of the supernatant were filtered through Amicon Centricon Plus-20 PL-30 filters with an approximate 30,000 molecular weight cutoff. Sr concentrations were determined by inductively coupled plasma spectrometry (ICP) and by inductively coupled plasma mass spectrometry (ICP-MS). At the end of, and at various times during the equilibration period, the solid phase present was separated from the solution and analyzed for total

chemical composition, and by X-ray diffraction (XRD) to ensure the presence of crystalline $SrCO_3$ [i.e., $SrCO_3$(c)]. $SrCO_3$(c) was the only phase identified and was present at the beginning and end of the equilibration period.

Experiments at higher temperatures, 50°C and 75°C, were conducted in the same general manner, except that the samples were prepared in the controlled atmosphere chamber, tightly capped, and then transferred to a thermostatic oven during the equilibration period. The tightly capped samples were withdrawn from the oven, returned to the inert atmosphere chamber, and sampled in the same general manner as at room temperature. The vials were opened inside the chamber and periodically measured for O_2 to determine if atmospheric gases had leaked into the samples. Precautions taken to minimize temperature change during sampling included: preheating all filters, tubes, and pipette tips to the appropriate temperature, placing the samples in a Styrofoam sample container to minimize heat loss, and pre-warming the centrifuge unit. Sample temperatures were monitored during this process, and the lowest observed final sample temperatures were 46.7°C for 50°C samples and 71.9°C for the 75°C samples. Since $SrCO_3$(c) shows a retrograde solubility as a function of temperature, such temperature changes would have resulted, in at most, an increase by a few percent in the observed Sr concentrations, even assuming instantaneous equilibration.

2.3 Thermodynamic Modeling

The aqueous thermodynamic model used in this study to interpret the solubility data was the ion-interaction model of Pitzer and coworkers (Pitzer 1973, 1991). This model emphasizes a detailed description of the specific ion interactions in the solution. The effects of the specific ion interactions on the excess solution free energy are contained within the expressions for the activity coefficients. The activity coefficients can be expressed in a general virial-type expansion as:

$$\ln \gamma_i = \ln \gamma_i^{DH} + \sum_j \beta_{ij}(I)\, m_j + \sum_j \sum_k C_{ijk}\, m_j\, m_k + \ \ldots \qquad (2.1)$$

where m is the molality and γ_iDH is a modified Debye-Hückel activity coefficient that is a universal function of ionic strength. $\beta_{ij}(I)$ and C_{ijk} are specific for each ion interaction and can be functions of ionic strength. Pitzer gives explicit phenomenological expressions for the ionic-strength dependence of β. The third virial coefficient, C, is taken to be independent of ionic strength. The form of β is different for like, unlike, and neutral ion interactions. A detailed description of the exact form of Eq. (2.1) is given elsewhere (Harvie et al. 1984; Felmy and Weare 1986; Felmy et al. 1989). The Pitzer thermodynamic model was used because it is applicable from zero to high concentration, and our solubility data extend to high ionic strength (I ~ 9m).

The Pitzer ion-interaction parameters were fit to the following temperature-dependent expression:

$$P(T) = a_1 + a_2T + a_3/T + a_4 \ln T + a_5/(T\text{-}263) + a_6T^2 + a_7/(680\text{-}T) + a_8/(T\text{-}227) \qquad (2.2)$$

where P(T) is a temperature-dependent ion-interaction parameter and T is in degrees Kelvin.

2.4 Results and Discussion

This section describes the $SrCO_3$(c) solubility data as a function of temperature and electrolyte composition, the development of the aqueous thermodynamic model describing Na^+-$EDTA^{4-}$ interactions, and our final thermodynamic model describing the Na-OH-CO_3-NO_3-EDTA-H_2O system.

2.4.1 $SrCO_3$(c) Solubility

The observed $SrCO_3$(c) solubilities in this study showed the same rapid equilibrations with time at higher temperature as seen previously by Felmy and Mason (1998) at lower temperature (Figure 2.1a,b). Increasing the $NaNO_3$ concentration in solution did tend to slow the equilibrations, the most notable example being at room temperature and at the highest added $NaNO_3$ concentration (5m), which did not appear to reach equilibrium or steady-state concentrations until the second sampling period at 36 days of equilibration (Figure 2.1c). The reasons for the slower rate of equilibration at higher $NaNO_3$ concentrations are unclear, but could be related to a slower net exchange of Sr^{2+} for Na^+ in the $EDTA^{4-}$ chelate or reduced interaction of the negative charged chelate with the $SrCO_3$(c) surface. In any event, the samples reached equilibrium or steady-state concentrations by the final sampling period. Therefore, only the analytical concentrations from the final sampling were used in the thermodynamic analysis and in the following discussion.

The addition of $NaNO_3$ results in reduced solubilities at all temperatures (see, for example, 50°C data, Figure 2.2). These reduced solubilities are at least partially explained by the competition of Na^+ for the $EDTA^{4-}$ chelate, as described in the next section. The effects of temperature (Figure 2.3) show the expected overall trend of decreasing solubility with increasing temperature, owing to the retrograde solubility of $SrCO_3$(c) with temperature (see Busenberg and Plummer 1984).

2.4.2 Thermodynamic Model Development

As a first attempt at developing a thermodynamic model to predict the observed solubilities at 25°C, we assembled the best thermodynamic data available from literature sources. This model included the solubility product for $SrCO_3$(c), formation constant for $SrEDTA^{2-}$, strontium carbonate aqueous complexes, and the Pitzer ion-interaction parameters for Na^+-$EDTA^{4-}$ (see Table 2.2). As expected, initial calculations using this model showed that the only important aqueous species present was the Sr-EDTA species ($SrEDTA^{2-}$). Neither the free Sr^{2+} cation nor the Sr-carbonate complexes were important species in these solutions. However, the calculated aqueous concentrations for the $SrEDTA^{2-}$ species do not show good agreement with the experimental data (Figure 2.4). The calculated solubilities at low carbonate concentration are consistently under-predicted, and the model predicts a large increase in solubility with increasing $NaNO_3$ concentration. This latter effect is clearly not observed in the experimental data. In fact, the effect of added electrolyte is, in general, opposite to this predicted trend (i.e., solubilities decrease with added electrolyte, see Figure 2.2). This trend of decreasing solubilities is not as apparent at 25°C, since the previous literature data in the absence of added $NaNO_3$ had a slightly different total chelate concentration.

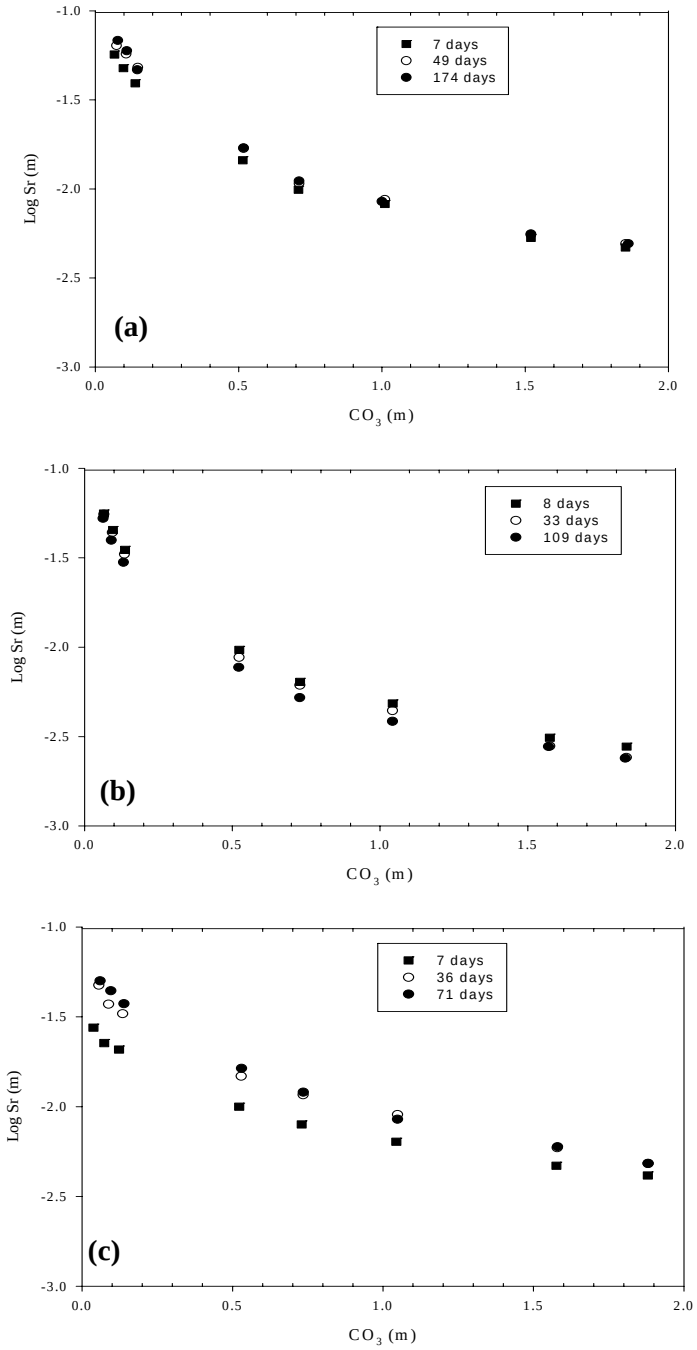

Figure 2.1. $SrCO_3$(c) Solubilities as a Function of Equilibration Time. (a) Room-temperature data from Felmy and Mason (1998) in the absence of $NaNO_3$. (b) 75°C data from this study in the absence of $NaNO_3$. (c) Room-temperature data from this study in the presence of 5m $NaNO_3$. EDTA concentration 0.1M.

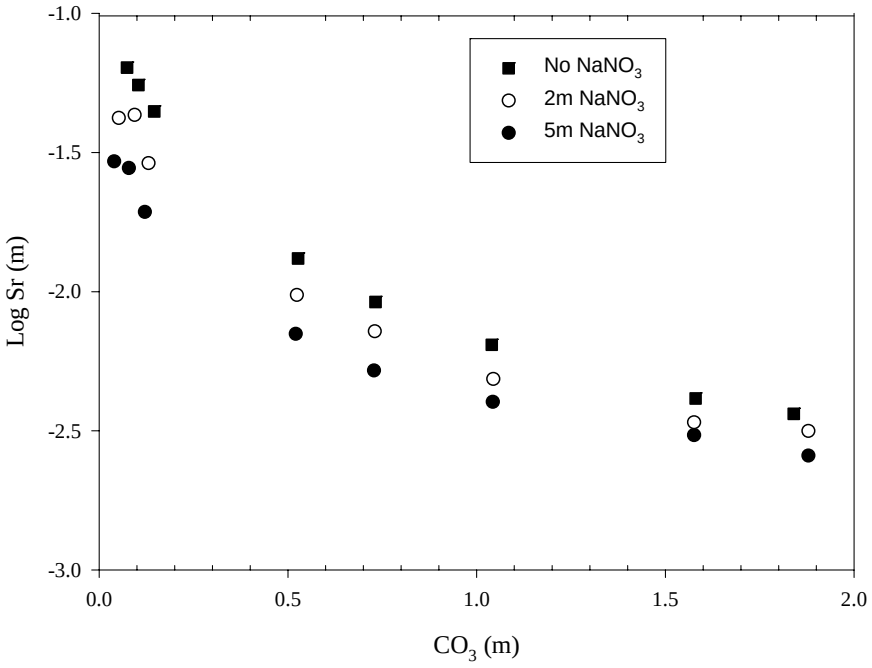

Figure 2.2. $SrCO_3$(c) Solubility Data Showing the Effects of Added $NaNO_3$ at 50°C. EDTA concentration 0.1M.

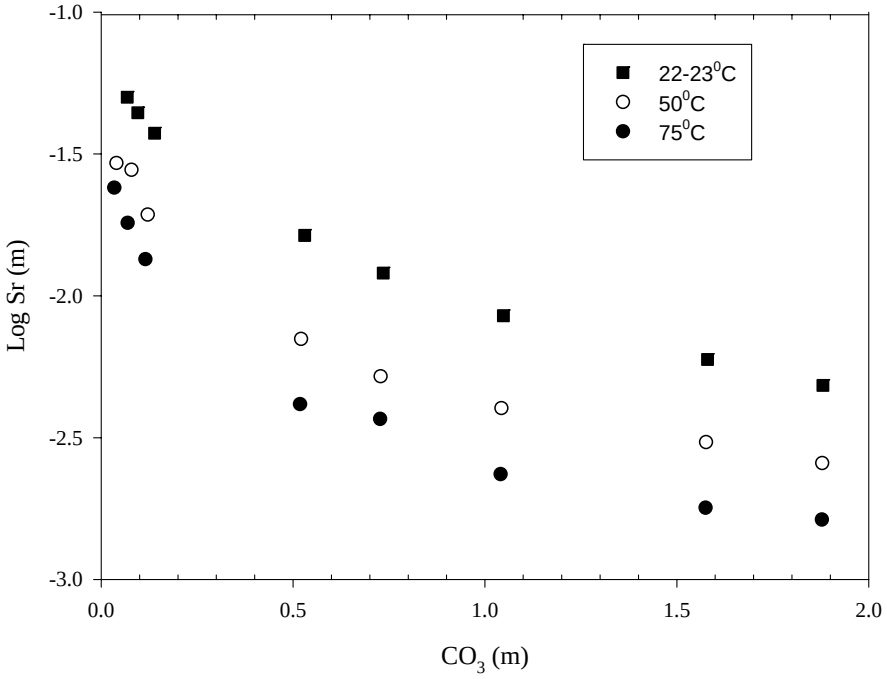

Figure 2.3. $SrCO_3$(c) Solubility Data Showing the Effects of Increasing Temperature in 5m $NaNO_3$ Solutions. EDTA concentration 0.1M.

Table 2.2. Initial Model Parameters Taken from the Literature

Parameter	Literature Source	Comments
$SrCO_3$(c) solubility product	Busenberg and Plummer (1984)	--
$SrCO_3$(aq) association reaction	Busenberg and Plummer (1984)	--
$Sr(CO_3)_2^{2-}$ association reaction	Felmy and Mason (1998)	--
$SrEDTA^{2-}$ association reaction	Martell and Smith (1995)	I = 0.1M
β^0, β^1,C^ϕ Na^+ - $EDTA^{4-}$	Mizera et al. (1999)	--
β^0, β^1,C^ϕ Sr^{2+}- OH^-	Felmy et al. (1998)	--
β^0 Na^+ - $Sr(CO_3)_2^{2-}$	Felmy et al. (1998)	--
β^0, β^1,C^ϕ Na^+ - CO_3^{2-}	Felmy et al. (1994)	Temperature coefficients fit from the data of Peiper and Pitzer (1982) from 25°C to 45°C.
β^0, β^1,C^ϕ Na^+ - NO_3^-	Felmy et al. (1994)	Fit to osmotic coefficient data from 25°C to 100°C.
β^0, β^1,C^ϕ Na^+ - OH^-		Fit to the temperature-dependent values of Pabalan and Pitzer (1987)
θ NO_3^- - CO_3^{2-}	Felmy and MacLean (2001)	Fit from the solubility data for $NaNO_3$-Na_2CO_3-H_2O at 25°C.

The most straightforward approach at this point was to begin with this literature-based model and adjust the necessary Pitzer ion-interaction parameters and standard-state equilibrium constants until a good fit to the experimental data was obtained. This effort quickly revealed two significant features required to obtain a good fit. First, as expected, the standard-state equilibrium constant for the $SrEDTA^{2-}$ association reaction needed to be greater than the simple reported value at I=0.1M. However, the calculated increase (0.8 log units) was significantly less than previous estimates for $CaEDTA^{2-}$ and $ZnEDTA^{2-}$ (see Table 2.2). The second required feature was the introduction of very large mixing terms for the $EDTA^{4-}$ species with the NO_3^- anion. While this latter effect was also expected, the magnitude of the required parameter (θ NO_3^-, $EDTA^{4-}$ = 0.33) was quite large in regard to the expected values for these parameters. In addition, this model did not explicitly recognize the expected strong association of Na^+ with the $EDTA^{4-}$ chelate. This association has been identified numerous times. Examples include: the nuclear magnetic resonance (NMR) data of James and Noggle (1969), the conditional protonation constants for $EDTA^{4-}$ and formation constants for $NaEDTA^{3-}$ (Daniele et al. 1985; Chen and Reid 1993) and inclusion of a $NaEDTA^{3-}$ ion association species in the interpretation of the enthalpy and heat capacity data for Na_4EDTA (Hovey et al. 1988). For these reasons, we elected to re-parameterize the Na_4EDTA system using the Pitzer model and including the $NaEDTA^{3-}$ species.

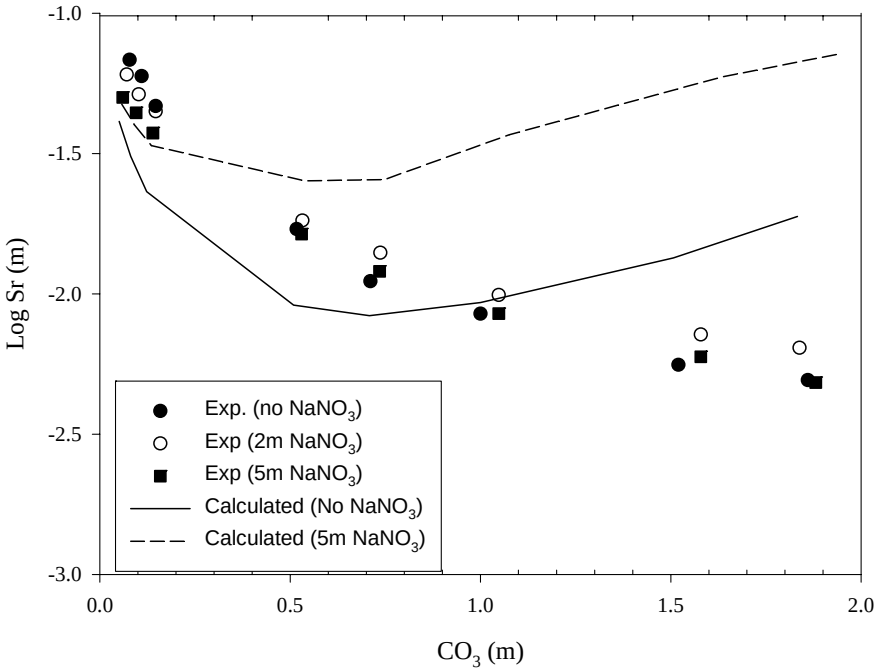

Figure 2.4. Experimental and Calculated Sr Concentrations at Room Temperature. Experimental data in the absence of $NaNO_3$ taken from Felmy and Mason (1998). Calculated concentrations utilize the parameters from the sources in Table 2.2.

To develop a model for the Na_4EDTA system, which included an ion pair, we elected to fit the apparent equilibrium constants for $H(EDTA)^{3-}/EDTA^{4-}$ protonation as a function of NaCl concentration reported by Mizera et al. (1999), along with the apparent equilibrium constants for $NaEDTA^{3-}$ formation reported by Daniele et al. (1985). In fitting the data of Mizera et al. (1999), we retained the ion-interaction parameters for Na^+-$HEDTA^{3-}$ used by Mizera et al. (1999) to ensure our model was also consistent with the other protonation reactions of EDTA as a function of added electrolyte. This fitting exercise resulted in calculation of the Pitzer ion-interaction parameters for Na^+ interactions with the $NaEDTA^{3-}$ species, as well as the standard-state equilibrium constant for the $NaEDTA^{3-}$ formation reaction. In addition, the ion-interaction parameters for Na^+-$EDTA^{4-}$ were evaluated (see Tables 2.3 and 2.4). A comparison between the model and experimental data is shown in Figure 2.5. This comparison also shows the data of Botts et al. (1965) for $EDTA^{4-}$ protonation. The data of Botts et al. (1965) serve as an independent test of the proposed model, since these results were not used in the model parameterization and extend to lower concentration. This comparison shows that the model extrapolates quite well to lower ionic strengths, even though the original data of Mizera et al. (1999) only went as low as 0.3M NaCl.

Utilizing this model with a $NaEDTA^{3-}$ species included, we re-fit the room-temperature data for $SrCO_3(c)$ solubility, adjusting the same set of parameters as for the case without including a $NaEDTA^{3-}$ species. The only difference was that the NO_3^- mixing term now involved the $NaEDTA^{3-}$ species rather than the $EDTA^{4-}$ species. The $EDTA^{4-}$ species was calculated to be at much lower concentration than the $NaEDTA^{3-}$ species. This new model also gave an excellent fit to the experimental data (Figure 2.6) and resulted in significantly lower mixing terms for the anionic ion interactions (i.e., θ NO_3^-, $NaEDTA^{3-}$ = 0.12) and a standard-state equilibrium constant for the $SrEDTA^{2-}$ formation reaction, which is 1.7 log

Table 2.3. Parameters for the Temperature-Dependent Expression (Eq. 2.1) for the Pitzer Ion-Interaction Parameters

Species	Parameter	a1	a2	a6	Reference
Na^+- CO_3^{2-}	β^0	-2.37265980e+00	1.42978840e-02	-2.08566020e-05	Felmy et al. (1994)
	β^1	-6.56843130e+00	5.18062300e-02	-8.20256870e-05	Felmy et al. (1994)
	C^ϕ	5.206000000e-03	0.0	0.0	Felmy et al. (1994)
Na^+- NO_3^-	β^0	-2.64744648e+00	1.52565224e-02	-2.13146667e-05	Felmy et al. (1994)
	β^1	-7.77643468e+00	4.58638400e-02	-6.34666667e-05	Felmy et al. (1994)
Na^+- OH^-	β^0	-6.60527020e-01	4.55226810e-03	-6.86137740e-06	See Table 2.2
	β^1	0.0	0.0	2.837918200e-06	See Table 2.2
	C^ϕ	1.046253000e-01	-5.6347570e-04	7.596489800e-07	See Table 2.2
Na^+- $EDTA^{4-}$	β^0	1.1	--	--	This Study
	β^1	15.6	--	--	This Study
	C^ϕ	0.001	--	--	Mizera et al. (1999)
Na^+ - $NaEDTA^{3-}$	β^0	0.59	--	--	This Study
	β^1	5.39	--	--	This Study
Na^+- $SrEDTA^{2-}$	β^0	0.3	--	--	This Study
	C^ϕ	-4.57312920e+00	2.89647688e-02	-4.55760000e-05	This Study
Na^+- $Sr(CO_3)_2^{2-}$	β^0	0.15	--	--	Felmy et al. (1998)
Na^+- $Ca(CO_3)_2^{2-}$	β^0	0.095	--	--	Felmy et al. (1998)
Na^+ - Sr^{2+}	θ	0.07	--	--	Felmy et al. (1998)
Sr^{2+}- OH^-	β^0	-0.061	--	--	Felmy et al. (1998)
	β^1	1.655	--	--	Felmy et al. (1998)
Ca^{2+}- OH^-	β^0	-0.1747	--	--	Harvie et al. (1984)
	β^1	-0.2303	--	--	Harvie et al. (1984)
	β^2	-5.72	--	--	Harvie et al. (1984)
OH^- - CO_3^{2-}	θ	0.1	--	--	Harvie et al. (1984)
OH^-- CO_3^{2-}-Na^+	ψ	-0.017	--	--	Harvie et al. (1984)
OH^- - NO_3^-	θ	-0.00005	--	--	Felmy et al. (1994)
NO_3^- - CO_3^{2-}	θ	0.14	--	--	Felmy and MacLean (2001)
NO_3^--$NaEDTA^{3-}$	θ	0.12	--	--	This Study

units higher than the reported value for the I=0.1M reference state. This increase is now in good agreement with previous estimates for $CaEDTA^{2-}$ (see Table 2.2). Including an explicit strong association for the Na^+ interaction with $EDTA^{4-}$ appears to improve the model by more directly accounting for the Na^+ competition for the EDTA chelate.

The model with the $NaEDTA^{3-}$ species included was also easier to extend over the required temperature, range, since the enthalpy and heat capacity data for this species calculated by Hovey et al. (1988) can be used directly. Although these data were only used to correct the standard-state equilibrium constant for formation of $NaEDTA^{3-}$, such variation in standard-state properties is frequently the largest source of

Table 2.4. Logarithms (Base 10) of the Thermodynamic Equilibrium Constants of Aqueous Phase Association Reactions and Solid Phase Dissolution Reactions (K_{sp}) Used in This Study

Species	Temperature (°C)	Log K^0	Reference
$SrEDTA^{2-}$	22-23	10.45	This Study
	50	10.36	This Study
	75	10.25	This Study
$NaEDTA^{3-}$	22-23	2.70	This Study
	50	2.60	This Study
	75	2.50	This Study
$CaEDTA^{2-}$	22-23	12.36	This Study
$SrCO_3(c)$	25	-9.27	Busenberg and Plummer (1984)
	50	-9.37	Busenberg and Plummer (1984)
	75	-9.59	Busenberg and Plummer (1984)
$CaCO_3(c)$	25	-8.41	Harvie et al. (1984)
$CaCO_3(aq)$	25	3.15	Harvie et al. (1984)
$SrCO_3(aq)$	25	2.81	Busenberg and Plummer (1984)
$Sr(CO_3)_2^{2-}$	25	3.31	Felmy et al. (1998)
$Ca(CO_3)_2^{2-}$	25	3.88	Felmy et al. (1998)
$NaNO_3(aq)$	25	-1.04	Felmy et al. (1994)
	50	-0.53	Felmy et al. (1994)
	75	-0.58	Felmy et al. (1994)

variation in the overall aqueous solution free energy. In these higher-temperature calculations, the variation in the solubility product of $SrCO_3(c)$ as a function of temperature was taken directly from Busenberg and Plummer (1984).

The 50°C and 75°C data sets were fit isothermally and the calculated parameters tested for consistency. The results showed that the standard-state equilibrium constant for $SrEDTA^{2-}$ formation reaction decreased in a roughly linear fashion over the temperature range 25°C to 75°C (see Table 2.4). This decrease is consistent with the previous studies of Carini and Martell (1954) over the temperature range 0°C to 30°C, which also showed a decrease in stability of the $SrEDTA^{2-}$ species with temperature. However, our calculated enthalpy change over the 25°C to 75°C range ($\Delta H° = -2.0$Kcal/mol) is less than that observed by Carini and Martell (1954) over the 0°C to 30°C temperature interval (i.e., $\Delta H° =$ -4.1Kcal/mol). The only other required parameters were β^0 for Na^+-$SrEDTA^{2-}$, C^ϕ for Na^+-$SrEDTA^{2-}$, and θ for NO_3^- -$NaEDTA^{3-}$. Of these ion-interaction parameters, only C^ϕ for Na^+-$SrEDTA^{2-}$ showed any

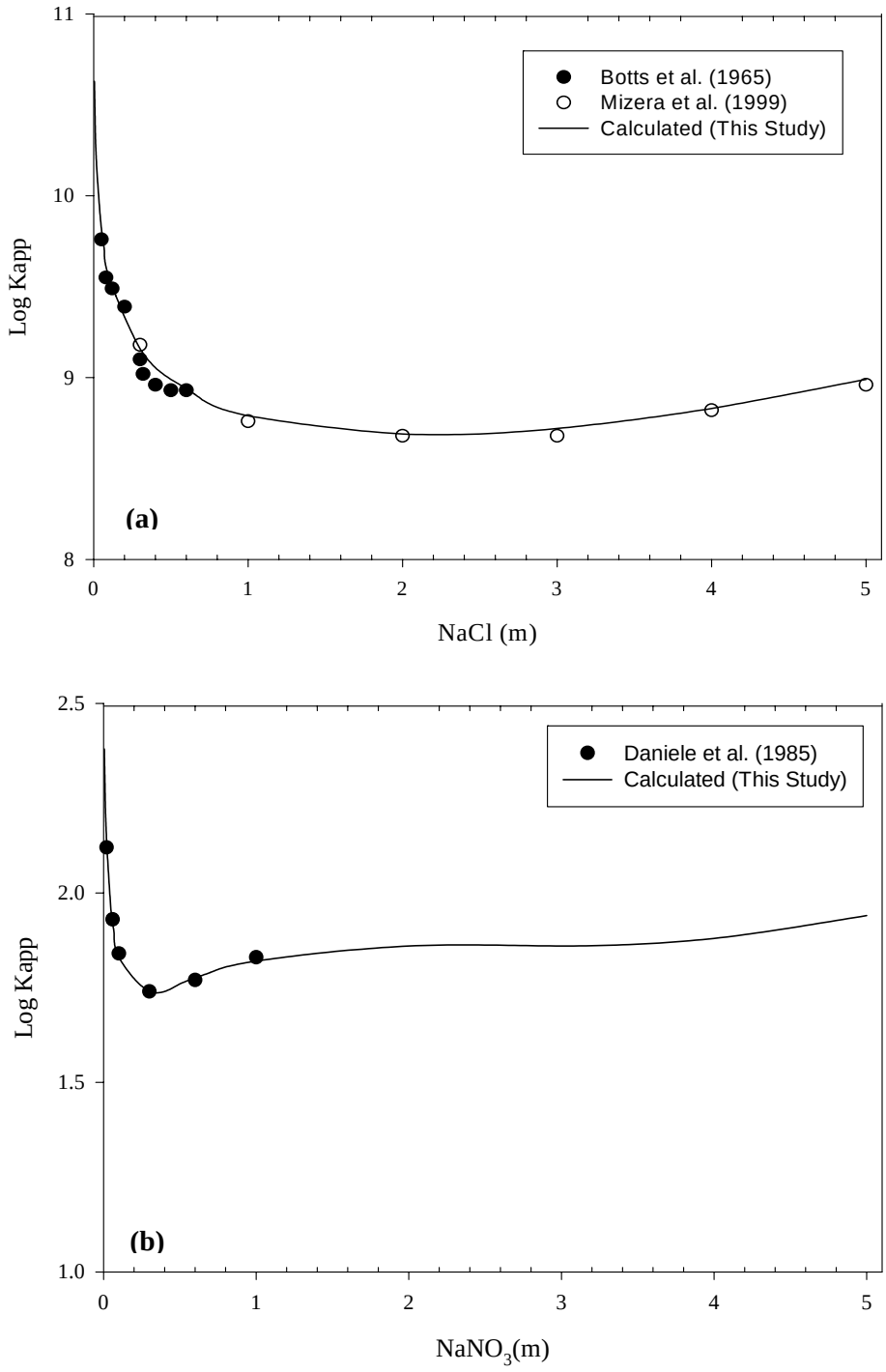

Figure 2.5. Experimental and Calculated Apparent Equilibrium Constants for (a) $H(EDTA)^{3-}/EDTA^{4-}$ and (b) $NaEDTA^{3-}$ Ion Association Constants

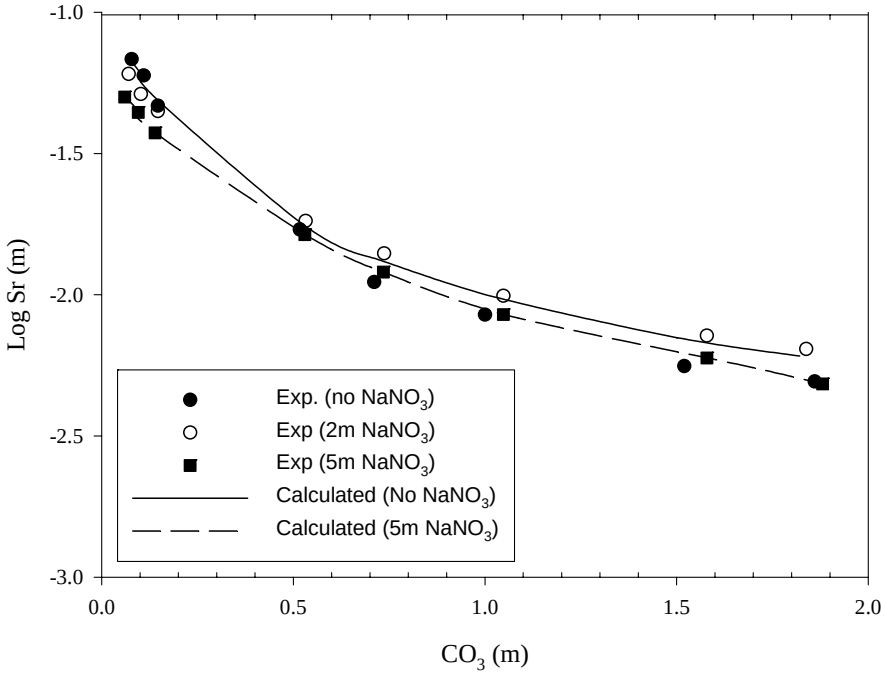

Figure 2.6. Experimental and Calculated Sr Concentrations at Room Temperature. Data in the absence of $NaNO_3$ taken from Felmy and Mason (1998)

significant temperature variation. As a result, both β^0 for Na^+-$SrEDTA^{2-}$ and θ for NO_3^- -$NaEDTA^{3-}$ were fixed at their 25°C values. The agreement between this final model and the experimental data at 50°C and 75°C is shown in Figure 2.7. The agreement between model and experiment is quite satisfactory. Tables 2.3 and 2.4 present a summary of the final model parameters used in this study.

2.4.3 Additional Model Applications

With an aqueous thermodynamic model developed for the Na-Sr-OH-CO_3-NO_3-EDTA-H_2O system, it is of interest to test this model on systems not used in model parameterization. Specifically, all of the studies just described have been conducted at one chelate concentration (0.1M), but it is of interest to test the applicability of the proposed model on a wide range of chelate concentrations. In addition, it has been hypothesized that the activity coefficients for divalent metal-EDTA complexes may be similar (Felmy and Mason 1998). If true, this would imply that the activity coefficient model proposed for $SrEDTA^{2-}$ might be applicable to other metal-EDTA chelates of similar charge. Both of these hypotheses are tested in this section. The data set used for comparison is our previous data on $SrCO_3$(c) solubility in the presence and absence of added $CaCO_3$(c) conducted at room temperature (Felmy and Mason 1998). The standard-state chemical equilibrium constant for $CaEDTA^{2-}$ was calculated by using the stability constant for $CaEDTA^{2-}$ given by Martell and Smith (1995) at I=0.1M combined with the same difference (+1.7 log units) found in this study for $SrEDTA^{2-}$ from the I=0.1M reference state to the standard state (see Table 2.4). The ion-interaction parameters for $SrEDTA^{2-}$ were also set to be identical to the $CaEDTA^{2-}$ values.

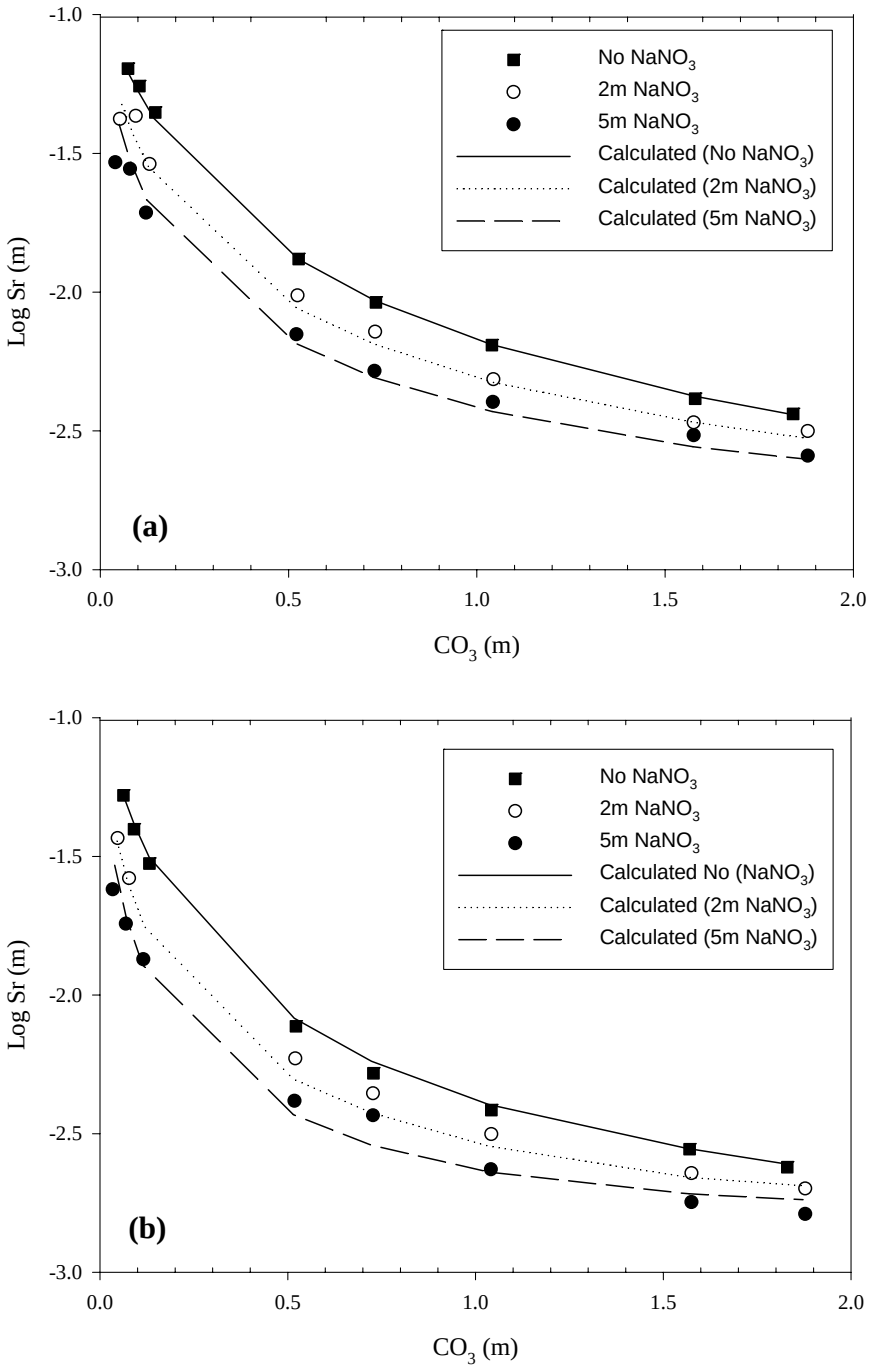

Figure 2.7. Experimental and Calculated Sr Concentrations at Higher Temperatures. (a) 50°C, (b) 75°C.

The calculated $SrCO_3$(c) solubilities as a function of added chelate concentration in both 0.1M Na_2CO_3 and 1.0M Na_2CO_3 show quite good agreement with all of the experimental data (Figure 2.8a), indicating the applicability of the proposed model to a wide range of chelate concentration. The model also quite accurately predicts the $CaCO_3$(c) solubilities in the presence of $SrCO_3$(c) (Figure 2.8b), indicating that the Pitzer parameters and the standard-state corrections for $SrEDTA^{2-}$ might be applicable to $CaEDTA^{2-}$ and potentially other chemical systems as well.

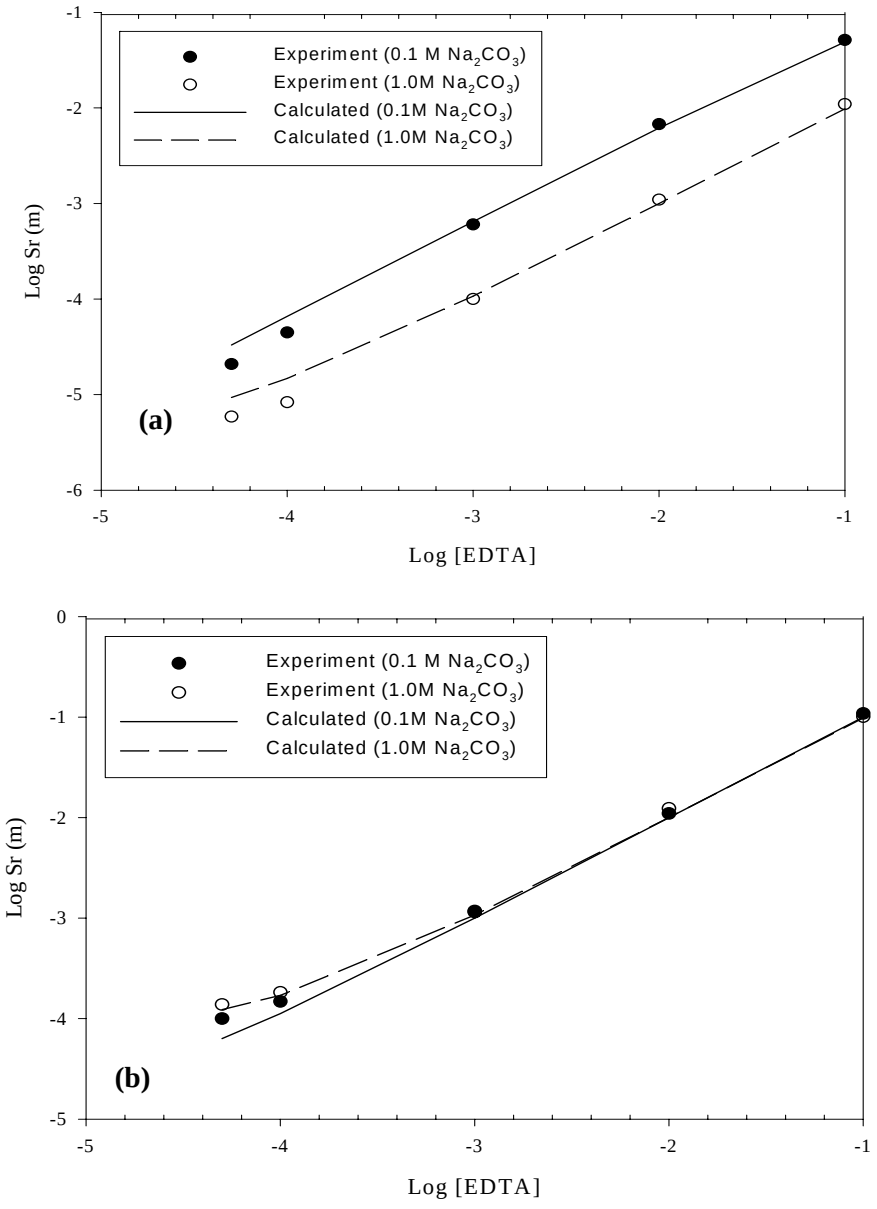

Figure 2.8. Experimental and Calculated $SrCO_3$(c) and $CaCO_3$(c) Solubilities as a Function of Chelate Concentration. (a) $SrCO_3$(c), (b) $CaCO_3$(c). Experimental data from Felmy and Mason (1998).

A more stringent test of the model is the calculation of the solubilities of $SrCO_3$(c) in the presence of $CaCO_3$(c). These results (Figure 2.9) also show quite satisfactory agreement between model and experiment, with the exception of the lowest two data points in 1.0M Na_2CO_3. In the case of these two points, the experimentally measured Sr concentrations are actually lower than in the absence of added chelate (compare with the dashed line for 1.0M Na_2CO_3). It is hard to explain how the addition of chelator could have resulted in lower $SrCO_3$(c) solubilities. Clearly, there is a problem with these two points not noticed before this detailed modeling analysis. However, the calculated concentrations using our present thermodynamic model appear to be reasonable given the known $SrCO_3$(c) solubilities in the absence of chelator.

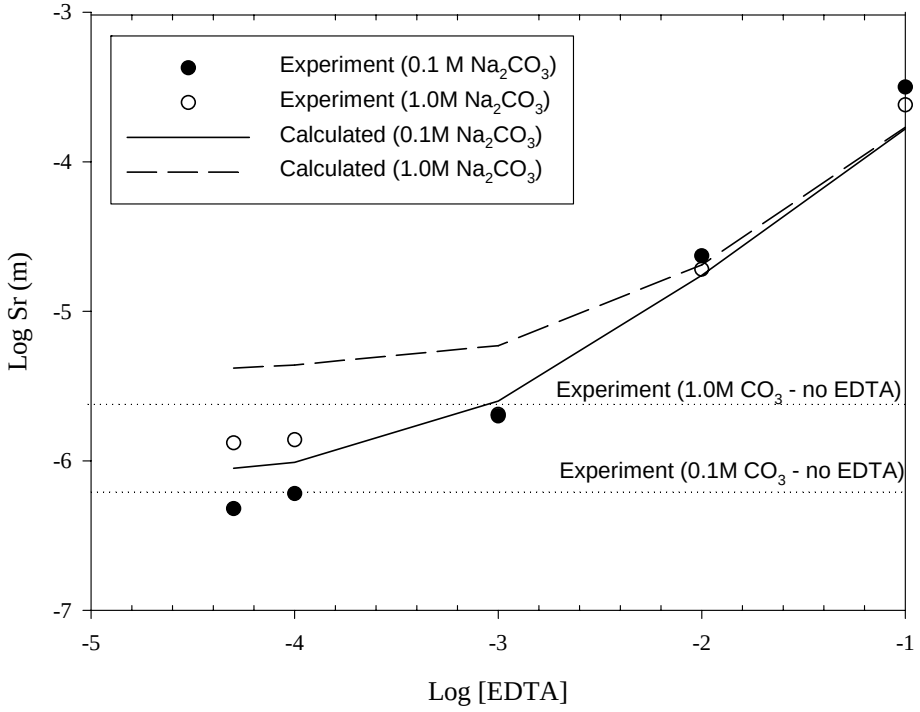

Figure 2.9. Experimental and Calculated $SrCO_3$(c) Solubilities as a Function of Chelate Concentration in the Presence of $CaCO_3$(c). Experimental data from Felmy and Mason (1998).

2.5 Summary

An aqueous thermodynamic model is proposed for the Na-Sr-OH-CO_3-NO_3-EDTA-H_2O system from 25°C to 75°C and across a broad range of ionic strengths (extending to ~9m). The model was developed from the analysis of literature data on apparent equilibrium constants, enthalpies, and heat capacities, as well as on an extensive set of solubility data on $SrCO_3$(c) in the presence of EDTA obtained as part of this study. The final aqueous thermodynamic model allows the extrapolation of standard-state equilibrium constants for these species, which are consistent with previous extrapolations for chemically similar species (i.e., $CaEDTA^{2-}$ and $ZnEDTA^{2-}$). The final model is then tested in chemical systems containing competing metal ions (i.e., Ca^{2+}) to further verify the proposed model and indicate the applicability of the model parameters to analogous chemical systems.

3.0 An Aqueous Thermodynamic Model for the Complexation of Strontium with HEDTA Valid to High Ionic Strength

This section describes the development of aqueous thermodynamic models for the complexation Sr^{2+} with HEDTA (Felmy et al. 2003). Work was focused on development of an aqueous thermodynamic model describing the effects of ionic strength (I), carbonate concentration, and temperature on the complexation of Sr^{2+} by HEDTA under basic conditions representative of tank waste. The thermodynamic model describing the Na^+ interactions with the $HEDTA^{3-}$ chelate relies solely on the use of Pitzer ion-interaction parameters. The exclusive use of Pitzer ion-interaction parameters differs significantly from our previous model for EDTA, which required the introduction of a $NaEDTA^{3-}$ ion pair. Estimation of the Pitzer ion-interaction parameters for $HEDTA^{3-}$ and $SrHEDTA^-$ with Na^+ allows the extrapolation of a standard-state equilibrium constant for the $SrHEDTA^-$ species, which is one order of magnitude greater than the 0.1M reference-state value available in the literature. The overall model was developed from data available in the literature on apparent equilibrium constants for HEDTA protonation, the solubility of salts in concentrated HEDTA solutions, and from new data on the solubility of $SrCO_3$(c) obtained as part of this study. The predictions of the final thermodynamic model for the Na-Sr-OH-CO_3-NO_3-HEDTA-H_2O system were tested by application to chemical systems containing competing metal ions (i.e., Ca^{2+}).

3.1 Background Literature

In contrast to the case for EDTA, little data exist from which to develop accurate thermodynamic models for the ionic strength (actually Na^+ concentration) dependence of the complexation of Sr^{2+} by $HEDTA^{3-}$. There are no published values for the Pitzer ion-interaction coefficients for Na^+ with the $HEDTA^{3-}$ uncomplexed species; there are only a few studies of the protonation reactions of $HEDTA^{3-}$ in Na^+-containing electrolytes (Bhat et al. 1967; Oyama et al. 1976); and there is only one study that extends to the high carbonate conditions typical of tank processing applications (Felmy and Mason 1998) at 25°C.

With these factors in mind, the specific objective of this study was to develop an aqueous thermodynamic model for the Na-Sr-OH-CO_3-NO_3-HEDTA-H_2O system that is valid over a range of temperatures (25°C to 75°C) and extended to high ionic strength (~9m). To achieve this objective, we tabulated literature data on the ionic strength dependence of the $HEDTA^{3-}$ protonation reactions and the solubility of $NaNO_3$(c) in the presence of high concentrations of HEDTA, and conducted new experimental studies on $SrCO_3$(c) solubility from room temperature to 75°C. $SrCO_3$(c) was selected for study, since it is likely to be the solubility-limiting phase in environmental (vadose zone) applications near leaking waste tanks and in waste tank processing applications designed to remove Sr-90.

3.2 Experimental Procedures and Thermodynamic Modeling

The experimental studies on the solubility of $SrCO_3$(c) at room temperature (22-23°C), 50°C, and 75°C were conducted as described in Felmy and Mason (2003), except that the HEDTA chelate was added as the reagent-grade trisodium salt. The solutions ranged in Na_2CO_3 concentration from 0.01M to 2.0M and in $NaNO_3$ concentration from 0 to 5m. The suspensions were equilibrated for up to 129 days. At the end

of the equilibration period, the solid phase present was separated from the solution and analyzed for total chemical composition, and by XRD to ensure the presence of $SrCO_3$(c). $SrCO_3$(c) was the only phase identified and was present at the beginning and end of the equilibration period.

The aqueous thermodynamic model used in this study to interpret the solubility data was the ion-interaction model of Pitzer and coworkers (Pitzer 1973, 1991), which was also described in Felmy and Mason (2003). The Pitzer ion-interaction parameters were fit to the following temperature-dependent expression:

$$P(T) = a_1 + a_2T + a_3/T + a_4\ln T + a_5/(T-263) + a_6T^2 + a_7/(680-T) + a_8/(T-227) \quad (3.1)$$

where P(T) is a temperature-dependent ion-interaction parameter and T is in degrees Kelvin.

3.3 Results and Discussion

This section describes the $SrCO_3$(c) solubility data as a function of temperature and electrolyte composition, the development of the aqueous thermodynamic model describing Na^+-$HEDTA^{3-}$ interactions, and our final thermodynamic model describing the Na-Sr-OH-CO_3-NO_3-HEDTA-H_2O system.

3.3.1 $SrCO_3$(c) Solubility

In general, the observed $SrCO_3$(c) solubilities in this study showed the same rapid equilibrations with time as found for EDTA in Felmy and Mason (2003). However, increasing the $NaNO_3$ concentration in solution did not measurably slow the equilibrations (Figure 3.1) as was found for EDTA. This more rapid rate of equilibration in the case of the lower charged $HEDTA^{3-}$ ion, relative to the $EDTA^{4-}$ ion, points to Na^+ binding as a factor in the equilibration rate. The stronger binding for Na^+ with the tetra-negative EDTA chelate apparently slows the rate of exchange with a divalent metal ion such as Sr^{2+}. The weaker binding of Na^+ for $HEDTA^{3-}$ is also indicated in the NMR data of James and Noggle (1969), which shows a Na^+ interaction with $HEDTA^{3-}$ that is significant but less than for $EDTA^{4-}$. This apparent weaker association may allow the development of a thermodynamic model that does not require the introduction of a $NaHEDTA^{2-}$ species. In any event, all of the samples reached equilibrium or steady-state concentrations in about 10 days.

The addition of $NaNO_3$ results in near constant to only slightly decreasing solubilities at all temperatures (Figure 3.2). This result also differs from the results for the EDTA chelate shown in Felmy and Mason (2003), where solubilities at 50°C and 75°C were significantly reduced upon the addition of $NaNO_3$. Again, this is a sign of a reduced interaction between Na^+ and $HEDTA^{3-}$ relative to Na^+ with $EDTA^{4-}$. The effects of temperature (Figure 3.3) show the expected overall trend of decreasing solubility with increasing temperature, owing to the retrograde solubility of $SrCO_3$(c) with temperature (see Busenberg and Plummer 1984).

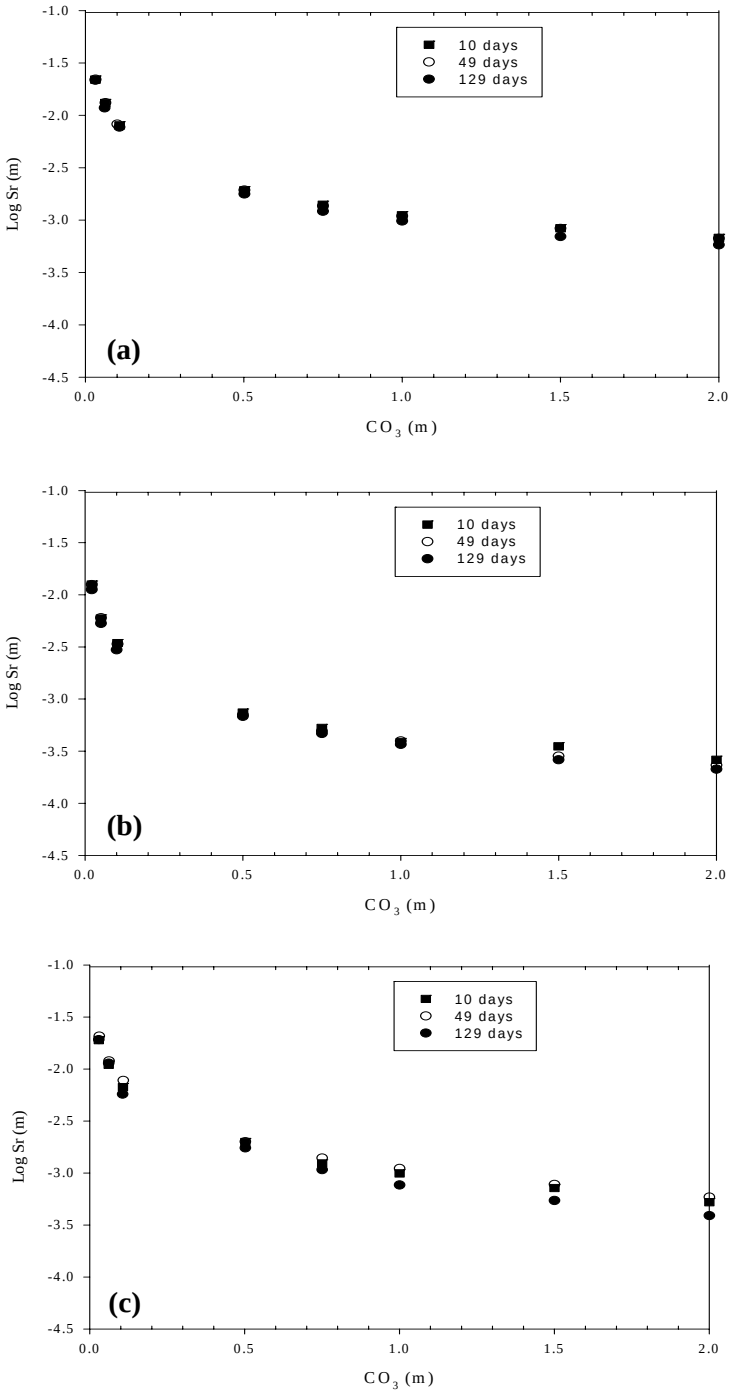

Figure 3.1. $SrCO_3$(c) Solubilities as a Function of Equilibration Time. (a) Room-temperature data in the absence of $NaNO_3$. (b) 75°C data in the absence of $NaNO_3$. (c) Room-temperature data in the presence of 5m $NaNO_3$. HEDTA concentration 0.1M.

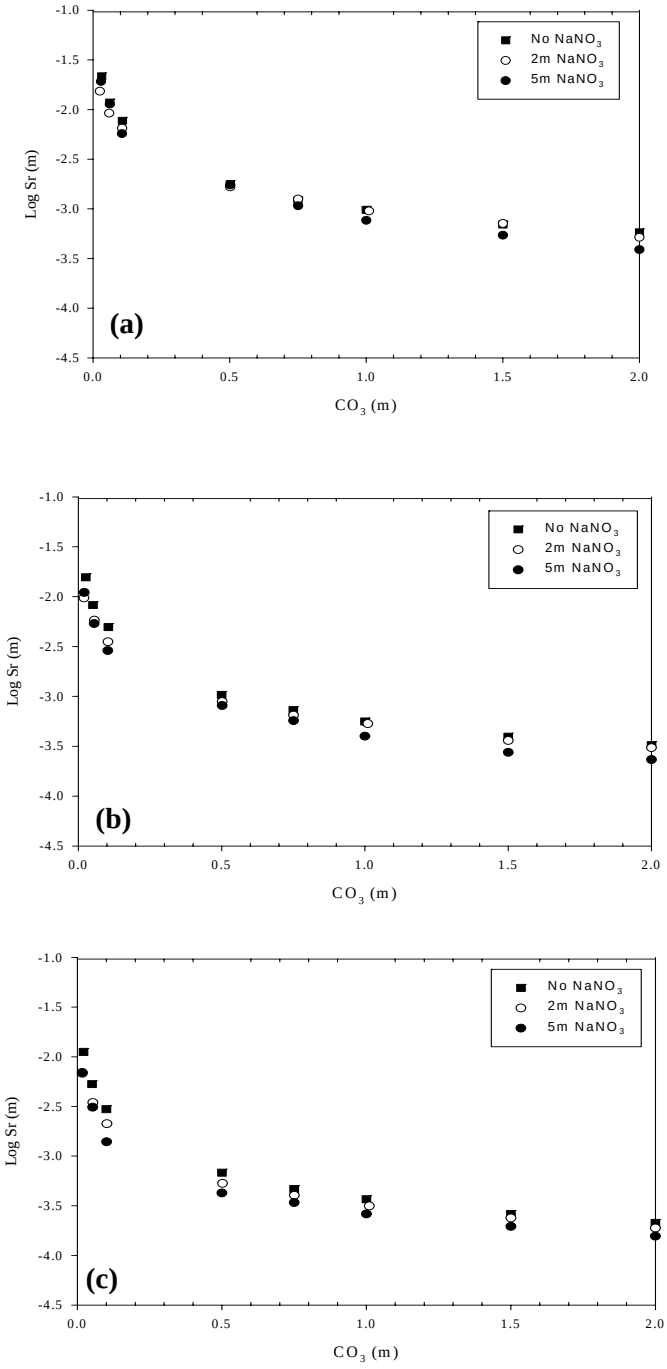

Figure 3.2. $SrCO_3$(c) Solubility Data Showing the Effects of Added $NaNO_3$ at Different Temperatures. (a) 25°C, (b) 50°C, (c) 75°C. HEDTA concentration 0.1M.

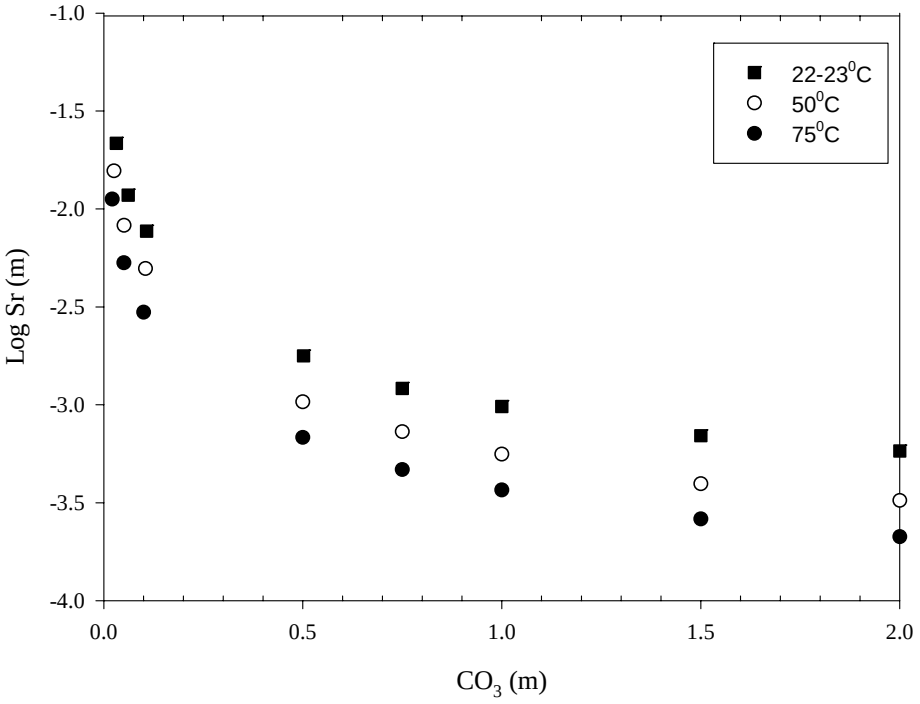

Figure 3.3. $SrCO_3$(c) Solubility Data Showing the Effects of Increasing Temperature in 5m $NaNO_3$ Solutions. HEDTA concentration 0.1M.

3.3.2 Thermodynamic Model Development

As a first attempt at developing a thermodynamic model to predict the observed solubilities at 25°C, we again began as in Felmy and Mason (2003) by assembling the best thermodynamic data available from literature sources. This model included the solubility product for $SrCO_3$(c), formation constant for $SrHEDTA^-$, and formation constants and ion-interaction parameters for strontium carbonate aqueous complexes (Table 3.1).

Two sets of these parameters deserve special comment. First, the formation constant for $SrHEDTA^-$ (Log K = 6.8) was taken directly from Martell and Smith (1995) at an ionic strength of 0.1M. Second, there are no published values for the Pitzer ion-interaction parameters for Na^+-$HEDTA^{3-}$. These values were estimated from the corresponding values for EDTA species of the same charge, i.e., Na^+-$H(EDTA)^{3-}$ where, in this case, $H(EDTA)^{3-}$ refers to the mono-protonated form of EDTA. As expected, the only important aqueous species calculated to be present was the complexed $SrHEDTA^-$ ion. Surprisingly, this initial model gave relatively uniform predictions of the solubility of $SrCO_3$(c) as a function of added Na_2CO_3 and, in fact, fairly accurately predicted the small differences in solubility resulting from the addition of $NaNO_3$ (Figure 3.4). The major error in this model appears to be the use of the formation constant for $SrHEDTA^-$ at the I=0.1M value. As we have previously shown for EDTA, the required standard-state formation constants can be significantly higher than the reported I=0.1M values. We therefore, fit the equilibrium constant for formation of the $SrHEDTA^-$ species to the three data points at the lowest Na_2CO_3 concentration and in the absence of $NaNO_3$. This estimated standard-state equilibrium

Table 3.1. Initial Model Parameters Taken from the Literature

Parameter	Literature Source	Comments
$SrCO_3$(c) solubility product	Busenberg and Plummer (1984)	--
$SrCO_3$(aq) association reaction	Busenberg and Plummer (1984)	--
$Sr(CO_3)_2^{2-}$ association reaction	Felmy and Mason (1998)	--
$SrHEDTA^-$ association reaction	Martell and Smith (1995)	I = 0.1M
β^0, β^1,C^ϕ Na^+ - $HEDTA^{3-}$	Estimated from sodium EDTA analog	EDTA analog data from Mizera et al. (1999)
β^0, β^1,C^ϕ Sr^{2+}- OH^-	Felmy et al. (1998)	--
β^0 Na^+ - $Sr(CO_3)_2^{2-}$	Felmy et al. (1998)	--
β^0, β^1,C^ϕ Na^+ - CO_3^{2-}	Felmy et al. (1994)	Temperature coefficients fit from the data of Peiper and Pitzer (1982) from 25°C to 45°C.
β^0, β^1,C^ϕ Na^+ - NO_3^-	Felmy et al. (1994)	Fit to osmotic coefficient data from 25°C to 100°C.
β^0, β^1,C^ϕ Na^+ - OH^-	--	Fit to the temperature-dependent values of Pabalan and Pitzer (1987)
θ NO_3^- - CO_3^{2-}	Felmy and MacLean (2001)	Fit from the solubility data for $NaNO_3$-Na_2CO_3-H_2O at 25°C.

constant (Log K^0 = 7.67) is approximately 0.9 log units greater than the reported value at I=0.1M. This estimate is consistent with the overall experimental solubilities, which are approximately a log unit greater than the initial calculated values; see Figure 3.4. However, since the initial differences between calculated and experimental solubilities are not exactly uniform as a function of added Na_2CO_3, a simple adjustment of the standard-state equilibrium constant does not accurately predict the entire 25°C data set (see Figure 3.4, Log K^0 adjusted calculations). Nevertheless, this simple analog model combined with the use of a standard-state log equilibrium constant of 7.67 for the formation of the $SrHEDTA^-$ species predicts the solubility of $SrCO_3$(c) at room temperature within experimental error to a Na_2CO_3 concentration of at least 0.5m.

However, the ion-interaction parameters between Na^+ and the $SrHEDTA^-$ chelate species have been set to zero in these calculations. These ion-interaction parameters are mathematically redundant with the Na^+-$HEDTA^{3-}$ parameters, in the $SrCO_3$(c) data set, owing to the mass balance constraint between the uncomplexed $HEDTA^{3-}$ species and the $SrHEDTA^-$ species. It is therefore impossible to determine a unique set of ion-interaction parameters for both the $HEDTA^{3-}$ and the $SrHEDTA^-$ species from the $SrCO_3$(c) solubility data alone. This parameter degeneration is most easily addressed by analyzing data in the Na^+-$HEDTA^{3-}$-H_2O system in the absence of any complexed metal ions.

Unfortunately, as described in the introduction, there are only a few studies involving the Na^+-$HEDTA^{3-}$-H_2O system that can be used to estimate Pitzer ion-interaction parameters for the Na^+-$HEDTA^{3-}$ ion interactions. These studies include the apparent equilibrium constants for $HEDTA^{3-}$ protonation given by

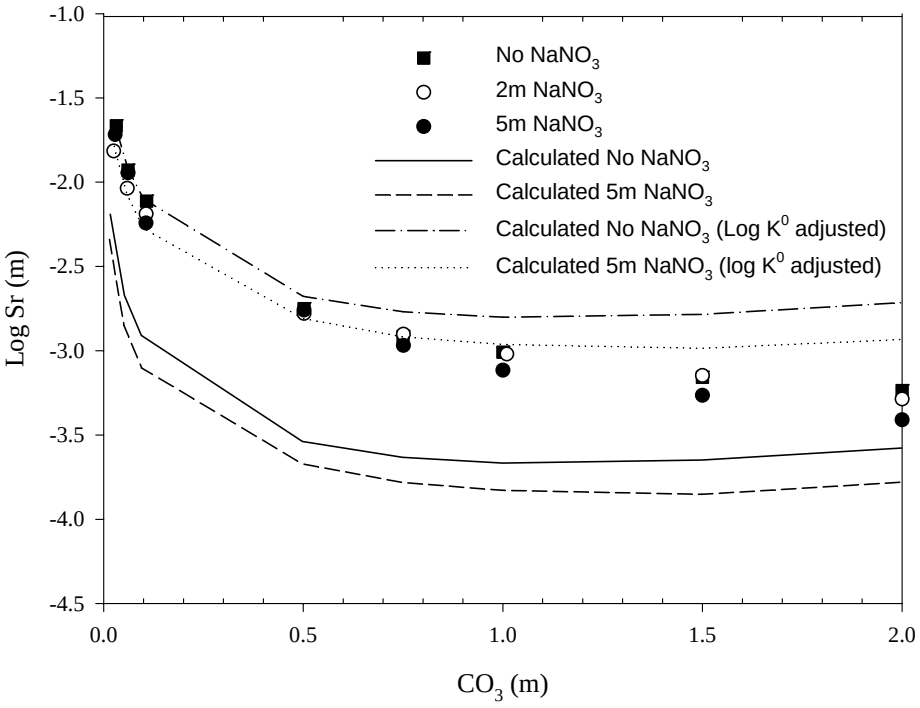

Figure 3.4. Experimental and Calculated Sr Concentrations at Room Temperature. Calculated concentrations utilize the parameters from the sources in Table 3.1. The notation, Log K^0 adjusted, refers to increasing the standard-state equilibrium constant for the $SrHEDTA^-$ species as described in the text.

Bhat et al. (1967) and Oyama et al. (1976) determined in 0.2M and 1.0M $NaClO_4$, respectively, and the solubility data for $NaNO_3$ and $Na_3HEDTA+2H_2O$ determined by Barney (1996) in concentrated Na_3HEDTA-$NaNO_3$-$NaNO_2$-NaOH-H_2O solutions.

Analysis of the apparent equilibrium constant data is complicated both by the need to examine the equilibrium constants for all three $HEDTA^{3-}$ protonation reactions and by the fact that data are available for only two ionic strengths. Analysis of the solubility data of Barney (1996) is complicated by the extremely concentrated nature of the solutions (Na concentrations from 14 to 17m) and the presence of multiple anions in the solution (NO_3^-, NO_2^-, OH^-, and $HEDTA^{3-}$). Nevertheless, these are apparently the only data that can be used to establish a set of Na^+-$HEDTA^{3-}$ ion-interaction parameters that are independent of the reactions with the metal ions.

We began by analyzing the apparent equilibrium constant data of Bhat et al. (1967) and Oyama et al. (1976) in 0.2M and 1.0M $NaClO_4$. In analyzing these data the only binary Na^+-$H_x(EDTA^{3-x})$ parameters that affect the final result are β^0 and β^1. The C^ϕ parameter is important only at higher ionic strengths. Also, only two parameters can be mathematically determined, since there are data available at only two ionic strengths. In this regard, we elected to determine the standard-state equilibrium constant for each protonated HEDTA species and the corresponding value of β^0 for Na^+-$H_x(HEDTA)^{3-x}$. The β^1 parameter was locked in at the Na^+-$H_x(EDTA)^{4-x}$ value given by Mizera et al. (1999) for the corresponding EDTA species of the same charge. Also, in agreement with Mizera et al. (1999), all interaction parameters for

the neutral $H_3HEDTA(aq)$ species were set to zero. This analysis yielded the following values for the ion-interaction parameters: β^0 for Na^+-$H_2(HEDTA)^-$ = -0.38, β^0 for Na^+-$H(HEDTA)^{2-}$ = 0.21, and β^0 for Na^+-$HEDTA^{3-}$ = 0.23. These values compare with the corresponding values for EDTA species of the same charge of β^0 for Na^+-H_3EDTA^- = -0.256, β^0 for Na^+-H_2EDTA^{2-} = -0.1262, and β^0 for Na^+-$HEDTA^{3-}$ = 0.5458. Of these calculated values only the value determined from the second protonation reaction appears discordant, as a result of the unusual behavior of the apparent equilibrium constant for the second proton dissociation constant for HEDTA, which decreases with increasing electrolyte concentration. This irregularity has been noted in the past and attributed to a "partial esterification" of the HEDTA (see Merciny et al. 1976 for discussion). From this analysis, we adopted the value β^0 for Na^+-$HEDTA^{3-}$ = 0.23.

With the value of β^0 for Na^+-$HEDTA^{3-}$ determined, we examined the solubility data of Barney (1996) for $NaNO_3(c)$ in mixed electrolytes. As previously mentioned, these data are at very high electrolyte concentration and contain several anions in solution. Therefore, our objective was simply to determine the most important ion-interaction parameters in this data set and check the magnitude of the calculated parameters to determine if these values were consistent with previously published values for similar electrolyte types. With these factors in mind, a satisfactory fit at 25°C (see Figure 3.5) to the $NaNO_3(c)$ solubility data could be obtained by adjusting the values of C^ϕ for Na^+-$HEDTA^{3-}$ = -0.014 and θ for $HEDTA^{3-}$ NO_3^- = 0.17. The value of C^ϕ for Na^+-$HEDTA^{3-}$ compares with the values of C^ϕ for Na^+-$H(EDTA)^{3-}$ = -0.048, and C^ϕ for Na^+-$Citrate^{3-}$ = 0.047 published by Mizera et al. (1999). The calculated value of C^ϕ for Na^+-$HEDTA^{3-}$ = -0.014 certainly falls within this expected range. The value of θ for $HEDTA^{3-}$ NO_3^- = 0.17 compares with our value of θ for $NaEDTA^{3-}$-NO_3^- = 0.12 (Felmy and Mason 2003), and consequently, would also appear reasonable. It should also be noted that the data reported in Figure 3.5 were also saturated with respect to $Na_3HEDTA{+}2H_2O$. However, no solubility products were available for this phase.

Using the described thermodynamic model, we estimated a standard-state equilibrium constant for the dissolution reaction of this phase to be Log K^0 = 0.11. This value gives a good representation of the solubility of $Na_3HEDTA{+}2H_2O$ (maximum error 13% in the predicted concentration of $HEDTA^{3-}$, data not shown). The parameters determined from fitting the $NaNO_3(c)$ solubility data are at least consistent with the $Na_3HEDTA{+}2H_2O$ solubility as well.

The $SrCO_3(c)$ data were then re-analyzed to determine if the data could be explained using this revised parameter set for Na^+-$HEDTA^{3-}$. This analysis required the adjustment only of β^0 for Na^+-$SrHEDTA^-$, C^ϕ for Na^+-$SrHEDTA^-$, and the standard-state equilibrium constant for $SrHEDTA^-$ formation. The fit to the experimental data (Figure 3.6) was nearly exact. Interestingly, the new calculated equilibrium constant for $SrHEDTA^-$ formation (Log K= 7.75) compares very favorably with the initial estimate of Log K = 7.67 using exclusively analog ion-interaction parameters. Adjusting the Pitzer ion-interaction parameters did not dramatically affect the calculated standard-state equilibrium constant for $SrHEDTA^-$ formation. The correction between the reference-state value and the standard-state value is still approximately 1 log unit.

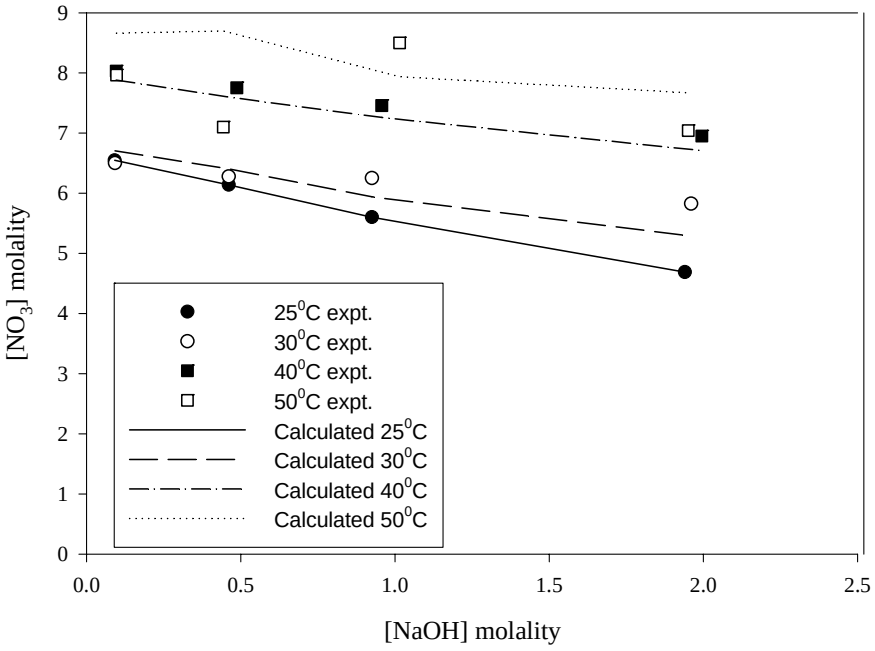

Figure 3.5. Experimental and Calculated $NaNO_3$(c) Solubilities in Mixed Electrolyte Solutions at Room Temperature. Experimental data of Barney (1996).

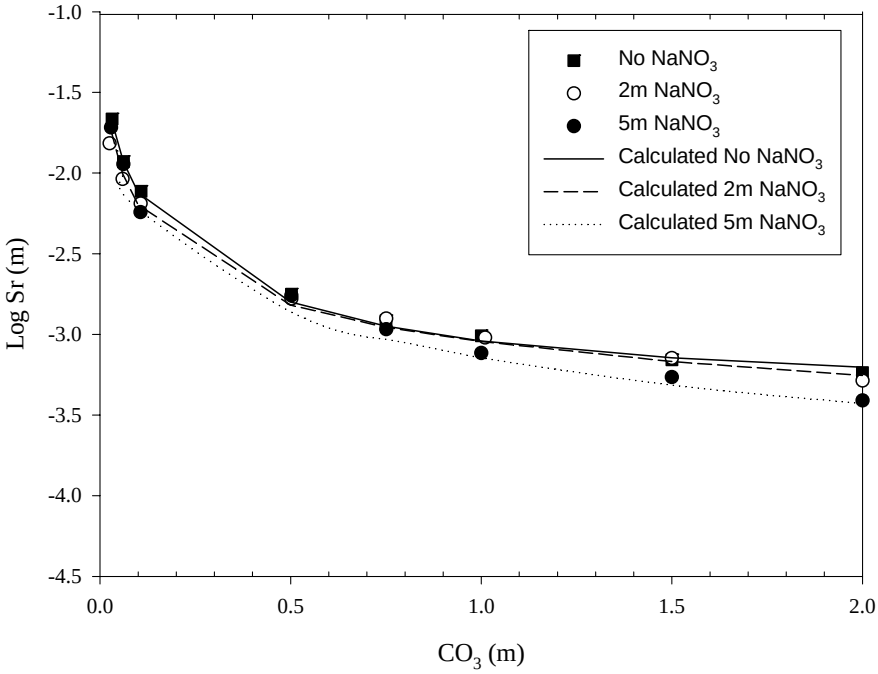

Figure 3.6. Experimental and Calculated Sr Concentrations at Room Temperature. Model parameters used in these calculations are given in Tables 3.2 and 3.3.

Table 3.2. Parameters for the Temperature-Dependent Expression (Eq. 3.1) for the Pitzer Ion-Interaction Parameters

Species	Parameter	a1	a2	a6	Reference
Na^+- CO_3^{2-}	β^0	-2.37265980e+00	1.42978840e-02	-2.08566020e-05	Felmy et al. (1994)
	β^1	-6.56843130e+00	5.18062300e-02	-8.20256870e-05	Felmy and Mason (2003)
	C^ϕ	5.206000000e-03	0.0	0.0	Felmy and Mason (2003)
Na^+- NO_3^-	β^0	-2.64744648e+00	1.52565224e-02	-2.13146667e-05	Felmy and Mason (2003)
	β^1	-7.77643468e+00	4.58638400e-02	-6.34666667e-05	Felmy and Mason (2003)
Na^+- OH^-	β^0	-6.60527020e-01	4.55226810e-03	-6.86137740e-06	See Table 3.1
	β^1	0.0	0.0	2.837918200e-06	Felmy and Mason (2003)
	C^ϕ	1.046253000e-01	-5.6347570e-04	7.596489800e-07	Felmy and Mason (2003)
Na^+-HEDTA $^{3-}$	β^0	0.23	--	--	This Study
	β^1	5.22	--	--	EDTA charge analog Mizera et al. (1999)
	C^ϕ	-0.479114	0.00156	--	This Study
Na^+- SrHEDTA $^-$	β^0	0.62482	-0.0028	--	This Study
	β^1	0.29	--	--	EDTA charge analog Mizera et al. (1999)
	C^ϕ	-0.32778	0.0012		This Study
Na^+- $Sr(CO_3)_2^{2-}$	β^0	0.15	--	--	Felmy et al. (1998)
Na^+- $Ca(CO_3)_2^{2-}$	β^0	0.095	--	--	Felmy and Mason (2003)
Na^+ - Sr^{2+}	θ	0.07	--	--	Felmy and Mason (2003)
Sr^{2+}- OH^-	β^0	-0.061	--	--	Felmy and Mason (2003)
	β^1	1.655	--	--	Felmy and Mason (2003)
Ca^{2+}- OH^-	β^0	-0.1747	--	--	Harvie et al. (1984)
	β^1	-0.2303	--	--	Felmy and Mason (2003)
	β^2	-5.72	--	--	Felmy and Mason (2003)
OH^- - CO_3^{2-}	θ	0.1	--	--	Harvie et al. (1984)
OH^-- CO_3^{2-}- Na^+	ψ	-0.017	--	--	Harvie et al. (1984)
OH^- - NO_3^-	θ	-0.00005	--	--	Felmy et al. (1994)
NO_3^- - CO_3^{2-}	θ	0.14	--	--	Felmy and MacLean (2001)
NO_3^-- $HEDTA^{3-}$	θ	0.17	--	--	This Study

Table 3.3. Logarithms (Base 10) of the Thermodynamic Equilibrium Constants of Aqueous Phase Association Reactions and Solid Phase Dissolution Reactions (K_{sp}) Used in This Study

Species	Temperature (°C)	Log K^0	Reference
$SrHEDTA^-$	22-23	7.75	This Study
	50	7.67	Felmy and Mason (2003)
	75	7.60	Felmy and Mason (2003)
$CaHEDTA^-$	22-23	9.20	Felmy and Mason (2003)
$SrCO_3(c)$	25	-9.27	Busenberg and Plummer (1984)
	50	-9.37	Felmy and Mason (2003)
	75	-9.59	Felmy and Mason (2003)
$CaCO_3(c)$	25	-8.41	Harvie et al. (1984)
$CaCO_3(aq)$	25	3.15	Felmy and Mason (2003)
$SrCO_3(aq)$	25	2.81	Busenberg and Plummer (1984)
$Sr(CO_3)_2^{2-}$	25	3.31	Felmy et al. (1998)
$Ca(CO_3)_2^{2-}$	25	3.88	Felmy and Mason (2003)
$NaNO_3(aq)$	25	-1.04	Felmy et al. (1994)
	50	-0.53	Felmy and Mason (2003)
	75	-0.58	Felmy and Mason (2003)

The advantage of this parameter set is that it reproduces the apparent protonation constants for HEDTA species and the solubility data in the presence of HEDTA, as well as the $SrCO_3(c)$ solubility data. New experimental data, particularly measurements of osmotic coefficients of Na^+-OH^--$HEDTA^{3-}$ solutions, would be required to more appropriately refine the set of parameters proposed here.

With a model available at 25°C, we examined the options for developing a temperature-dependent set of parameters. Unfortunately, the available data were even more limited than at 25°C. Specifically, no apparent equilibrium constants for the protonation of HEDTA in Na^+ solutions were found above 25°C. The organic solubility data of Barney (1996) were available only at 25°C, 30°C, 40°C, and 50°C. Figure 3.5 shows that the 50°C data of Barney (1996) are badly scattered. This scatter is due to the wide ranges in the reported densities for these solutions. The inconsistencies in the reported densities result in large differences in the conversion factors between molarity to molality in these solutions. As a result, we analyzed the 40°C data isothermally, adjusting only the value of C^ϕ for Na^+-$HEDTA^{3-}$, the single most important parameter in the Barney data set. The calculated values of C^ϕ for Na^+-$HEDTA^{3-}$ at 25°C and 40°C were then fit to a linear temperature-dependent formalism, i.e., coefficients a1 and a2 (Eq. 3.1). All other parameters involving HEDTA were set to their 25°C values. This model was then used to predict the 30°C and 50°C data shown in Figure 3.5. The agreement appears satisfactory given the large scatter in the 50°C data set.

Next, the $SrCO_3$(c) solubility data as a function of temperature were analyzed. The solubility product for $SrCO_3$(c) was well known as a function of temperature, and we also had an estimate of the temperature dependence of the Na^+-$HEDTA^{3-}$ ion-interaction parameters to 50°C. Therefore, we were able to fit the $SrCO_3$(c) solubility data at 50°C, adjusting only the same parameters that were adjusted to fit the room-temperature data, i.e., β^0 for Na^+-$SrHEDTA^-$, C^ϕ for Na^+-$SrHEDTA^-$, and the standard-state equilibrium constant for the $SrHEDTA^-$ formation reaction. The agreement between the model and the experiment, as expected, is quite good (Figure 3.7a). As a partial test of this model, the parameters determined at room temperature and 50°C were then fit to a simple linear temperature-dependent expression. The $SrCO_3$(c) solubility data at 75°C were then predicted (Figure 3.7b). The agreement appears to be quite satisfactory.

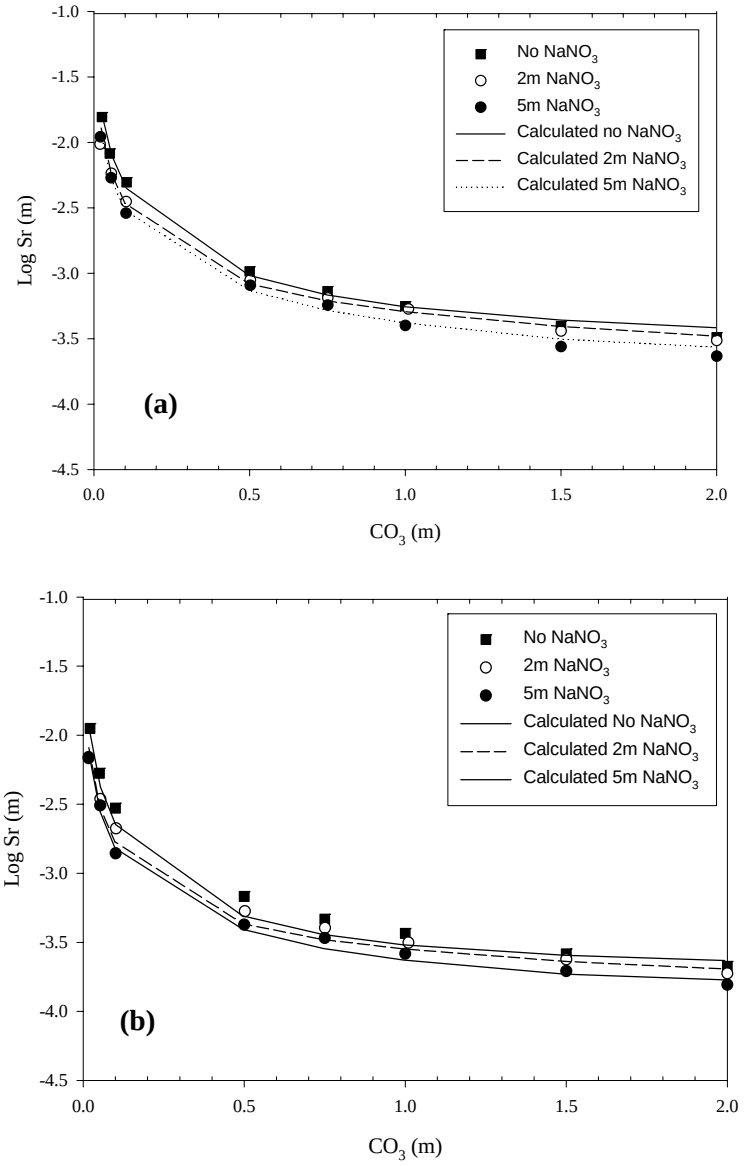

Figure 3.7. Experimental and Calculated Sr Concentrations at Higher Temperatures. (a) 50°C, (b) 75°C.

One final point: Martell and Smith (1995) recommend a value for the enthalpy of reaction for the formation of $SrHEDTA^-$ of -5.2Kcal/mol based on the calorimetric data of Wright et al. (1965) in 0.1M KNO_3. Our calculated standard-state enthalpy of reaction has the same sign, but is less (i.e., -1.3Kcal/mol). However, it was impossible to obtain a satisfactory fit to our $SrCO_3$(c) solubility data at higher temperatures using the 0.1M KNO_3 enthalpy value. The necessary adjustments to the Pitzer ion-interaction parameters to try to compensate for this difference always resulted in overall poor fits that included large and unrealistic ion-interaction parameters. Tables 3.2 and 3.3 present a summary of the final model parameters used in this study.

3.3.3 Additional Model Applications

As in Section 2.3 and Felmy and Mason (2003), a comparison is presented of our final model with experimental data for systems more complex than those used in model parameterization. The data set used for comparison is our previous data on $SrCO_3$(c) solubility in the presence and absence of added $CaCO_3$(c) conducted at room temperature (Felmy and Mason 1998). Again, as in Felmy and Mason (2003), the standard-state equilibrium constant for $CaHEDTA^-$ was calculated by using the stability constant for $CaHEDTA^-$ given by Martell and Smith (1995) at I=0.1M combined with the same difference (+1.0 log units) found in this study for $SrHEDTA^-$ from the I=0.1M reference state to the standard state (see Table 3.3). The ion-interaction parameters for $CaHEDTA^-$ were also set to be identical to the $SrHEDTA^-$ values.

The calculated $SrCO_3$(c) solubilities as a function of added chelate concentration in both 0.1M Na_2CO_3 and 1.0M Na_2CO_3, (Figure 3.8a), along with the calculated $CaCO_3$(c) solubilities in the presence of $SrCO_3$(c) (Figure 3.8b) are both in good agreement, indicating that the Pitzer parameters and the standard-state corrections for $SrHEDTA^-$ might be applicable to $CaHEDTA^-$ and potentially other chemical systems as well. In addition, the calculated $SrCO_3$(c) solubilities in the presence of $CaCO_3$(c) (Figure 3.9) show an overall satisfactory agreement between model and experiment.

3.4 Summary

An aqueous thermodynamic model is proposed for the Na-Sr-OH-CO_3-NO_3-HEDTA-H_2O system from 25°C to 75°C and across a broad range of ionic strengths (extending to ~9m). The model was developed from the analysis of literature data on apparent equilibrium constants, $NaNO_3$(c) solubilities in the presence of HEDTA, as well as on an extensive set of solubility data on $SrCO_3$(c) in the presence of HEDTA obtained as part of this study. The final aqueous thermodynamic model allows the extrapolation of standard-state equilibrium constants for the $SrHEDTA^-$ formation reaction that are approximately one order of magnitude greater than in their 0.1M reference state. A value for the equilibrium constant for the dissolution of $Na_3HEDTA{\cdot}2H_2O$ was also estimated. The final model was then tested in chemical systems containing competing metal ions (i.e., Ca^{2+}) to further verify the proposed model and indicate the applicability of the model parameters to analogous chemical systems.

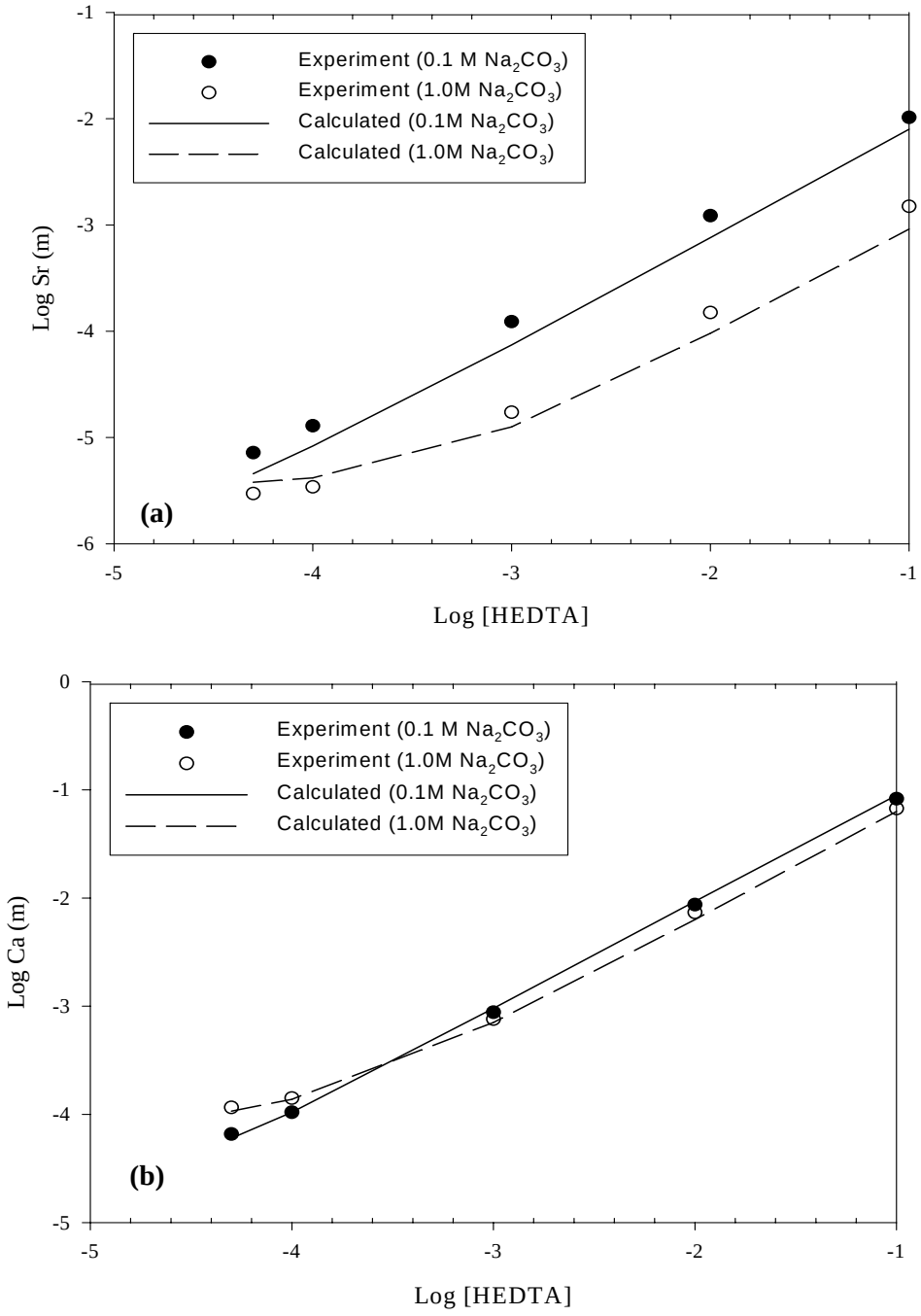

Figure 3.8. Experimental and Calculated $SrCO_3$(c) and $CaCO_3$(c) Solubilities as a Function of Chelate Concentration. (a) $SrCO_3$(c), (b) $CaCO_3$(c). Experimental data from Felmy and Mason (1998).

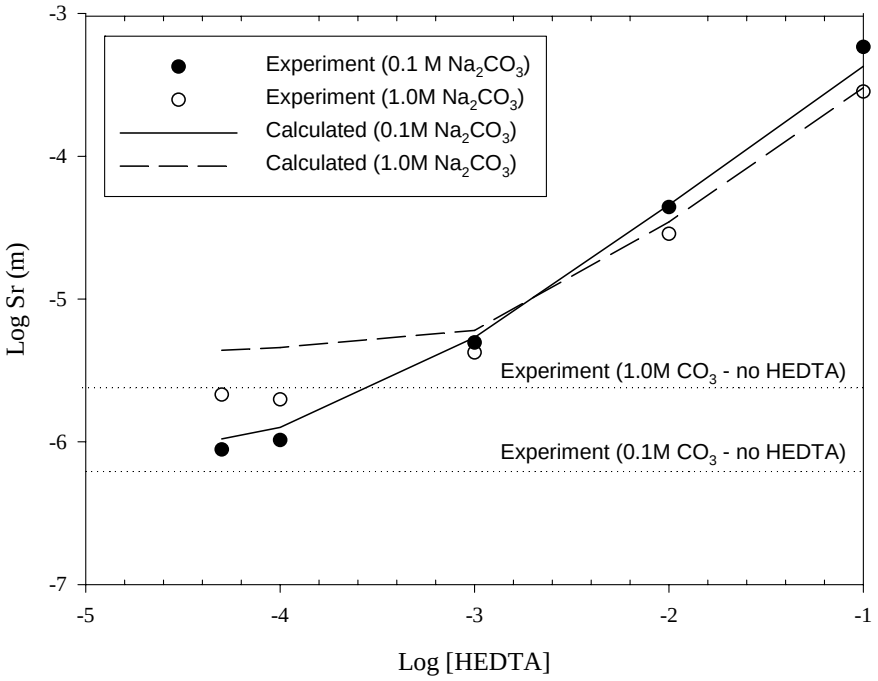

Figure 3.9. Experimental and Calculated $SrCO_3$(c) Solubilities as a Function of Chelate Concentration in the Presence of $CaCO_3$(c). Experimental data from Felmy and Mason (1998).

4.0 Calculation of Thermodynamic Values for Mn-Gluconate Complexes

This section describes the results from analysis of literature data on the complexation of Mn with gluconate. Thermodynamic parameters are calculated and are used to calculate the relative stability for various oxidation states of Mn, as well as compared to Fe, a major soluble component in AN-107 waste.

4.1 Background Literature

Experimental studies of the aqueous complexes of Mn(IV) and Mn(III) are extremely difficult, because of the simultaneous presence of multiple oxidation states in solution and the potential for complicating side reactions such as the precipitation of Mn(IV) oxides. The most precise data in the literature on the formation of Mn(III and IV)-gluconate complexes are the half-wave polarographic data of Bodini et al. (1976). Polarography is a useful technique for examining polyvalent metal ion systems, since the potential can be varied in a systematic manner generating both oxidation and reduction waves (see Kolthoff and Lingane 1952). The forward and reverse reactions can thus be checked for reversibility, a necessary criterion for interpreting such data in terms of thermodynamic models. The measurements are normally tabulated in terms of so-called half-wave potentials (i.e., the potential where half of the metal is the higher oxidation state and the other half is in the lower oxidation state). If these half-wave potentials are found to be reversible, the condition of thermodynamic equilibrium can be assumed.

Bodini et al. (1976) conducted a detailed study of the half-wave Kolthoff and Lingane (1952) potential for Mn(IV), Mn(III), and Mn(II) complexes under conditions of varying NaOH and sodium gluconate concentration. Bodini et al. (1976) concluded that at high base concentration (0.3M NaOH) and high gluconate concentration (0.1M gluconate) all three oxidation states of Mn (II, III, and IV) were present as digluconate complexes with different numbers of associated hydroxyls. The Mn(IV) complex was associated with three hydroxides; the Mn(III) complex was associated with one hydroxide; and the Mn(II) complex did not have any associated hydroxides. The associated one-electron transfer reactions and the experimental half-wave potentials are given in Table 4.1.

Table 4.1. Anodic Half Reactions and Half-Wave Potentials for Mn-Gluconate Reactions. Half-wave potentials are versus standard calomel electrode (SCE). Data of Bodini et al. (1976). The formula (GH_3) refers to the dianion of gluconate with the carboxylic acid and α-hydroxyl protons removed. V = volts, NHE = normal hydrogen electrode.

Reaction	$E_{½}$ (V) (SCE)	E^0(V) (NHE)
$Mn(IV)(GH_3)_2(OH)_3^{3-} + e^- \Leftrightarrow Mn(III)(GH_3)_2OH^{2-} + 2OH^-$	-0.27	0.765
$Mn(III)(GH_3)_2OH^{2-} + e^- \Leftrightarrow Mn(II)(GH_3)^{2-} + OH^-$	-0.53	0.495
$Mn(II)(GH_3)^{2-} + 2e^- \Leftrightarrow Mn(0) + 2GH_4^- + 2OH^-$	-1.75	-0.695

4.2 Calculation of Thermodynamic Parameters

Although these data are valuable in terms of species identification, they have certain limits with respect to determining precise thermodynamic data. First, the actual cell measurements were made using a reference Ag/AgCl cell with liquid junction that had been filled with tetramethylammonium chloride (TMAC). The TMAC concentration in the cell was adjusted to give a zero potential versus SCE. This calibration was necessary both to allow direct comparison of potential versus SCE and eliminate any Hg from the system (SCE contains Hg/Hg_2Cl_2), and to reduce the chloride concentration that could diffuse through the liquid junction. The introduction of Hg and the potential high chloride could interfere with the dropping Hg electrode measurements. A detailed example of the calculation of the equilibrium constants for the formation of Mn(IV), Mn(III), and Mn(II) complexes from the measured half-wave potentials is given in the appendix. The final calculated values are given in Table 4.2.

Table 4.2. Final Calculated Equilibrium Constants for Mn-Gluconate Complexation Reactions

Reaction	Log K^0
$Mn^{2+} + 2GH_4^- + 3H_2O \Leftrightarrow Mn(IV)(GH_3)_2(OH)_3^{3-} + 3H^+ + H_2(g)$	-51.78
$Mn^{2+} + 2GH_4^- + H_2O \Leftrightarrow Mn(III)(GH_3)_2OH^{2-} + 2H^+ + ½H_2(g)$	-24.85
$Mn^{2+} + 2GH_4^- \Leftrightarrow Mn(II)(GH_3)^{2-} + 2H^+$	-16.48

4.3 Application to Tank AN-107

The AN-107 diluted feed contains significant concentrations of gluconate (Table 4.3), which is chemically bound to ferric iron (note the similarities of the gluconate and iron concentrations in Table 4.3.) One interesting observation made by Hallen et al. (2000) is that iron hydroxides precipitate upon the addition of MnO_4^-. The reason for the appearance of the ferric hydroxide is presumed to be the displacement of the iron from the gluconate complex by reaction with the added Mn as the permanganate is reduced to lower oxidation states. However, which oxidation state the Mn is in when the displacement reaction occurs is unknown. It is therefore of interest to model the addition of MnO_4^- in AN-107 to help identify the possible oxidation states responsible for the displacement reaction and at least partially test the validity of the calculated thermodynamic data. In these calculations the thermodynamic data for ferric gluconate detailed by Felmy (2000) were used.

The results show that the formation of the Mn(IV)-containing species, $Mn(IV)(GH_3)_2(OH)_3^{3-}$, is the principal species formed in tank solutions with added permanganate (Figure 4.1). Interestingly, the calculated stability constant for this species is sufficiently strong to displace the ferric iron from the gluconate complex and precipitate ferric hydroxide, the observed phenomenon (Figure 4.2).

Table 4.3. AN-107 Diluted Feed Composition (from Felmy 2000)

Major Compounds	Concentration (m)	Minor Components	Concentration (m)	Organic Ligands[c]	Concentration (m)
Na^+	8.9	Al[b]	1.7×10^{-1}	Glycolate	0.30
NO_3^-	3.1	Ba[b]	3.4×10^{-5}	Gluconate[b]	0.022
NO_2^-	1.3	Ca[b]	1.3×10^{-2}	Citrate	0.055
CO_3^{2-}	1.6	Ce	2.3×10^{-4}	EDTA[b]	0.024
OH^-	0.84	Cd	4.9×10^{-4}	HEDTA[b]	0.0094
SO_4^{2-}	0.1	Cr[b]	3.3×10^{-3}	NTA[b]	0.037
PO_4^{3-}	0.037	Cs	1.1×10^{-4}	IDA	0.056
F^-[a]	0.39	Cu	3.9×10^{-4}		
Cl^-	0.046	Fe[b]	2.4×10^{-2}		
		K	3.8×10^{-2}		
		La[b]	1.9×10^{-4}		
		Mn[b]	2.3×10^{-3}		
		Nd[b]	5.8×10^{-4}		
		Ni[b]	7.9×10^{-3}		
		Pb	1.45×10^{-3}		
		Sr[b]	3.5×10^{-5}		
		U	3.6×10^{-4}		
		Zn	3.4×10^{-4}		
		Zr	5.6×10^{-4}		

(a) IC analysis probably includes formate and acetate.
(b) Metals for which thermodynamic data were included.
(c) Estimated from 9M simulant, assuming perfect dilution (i.e., 0.856).

4.4 Summary

The thermodynamic parameters for various Mn-gluconate complexes were calculated and then used to calculate the resulting impact on permanganate treatment of AN-107 waste, which has high levels of soluble metal ions, specifically Fe. The calculations predicted the observed behavior that, on permanganate additions and the subsequent reduction of Mn from 7 to lower oxidation states, the Mn displaces Fe from the complex, and the Fe precipitates from solution. Consequently, we conclude that the estimates of the Mn(II, III, and IV)-gluconate stability constants are useful for waste tank applications.

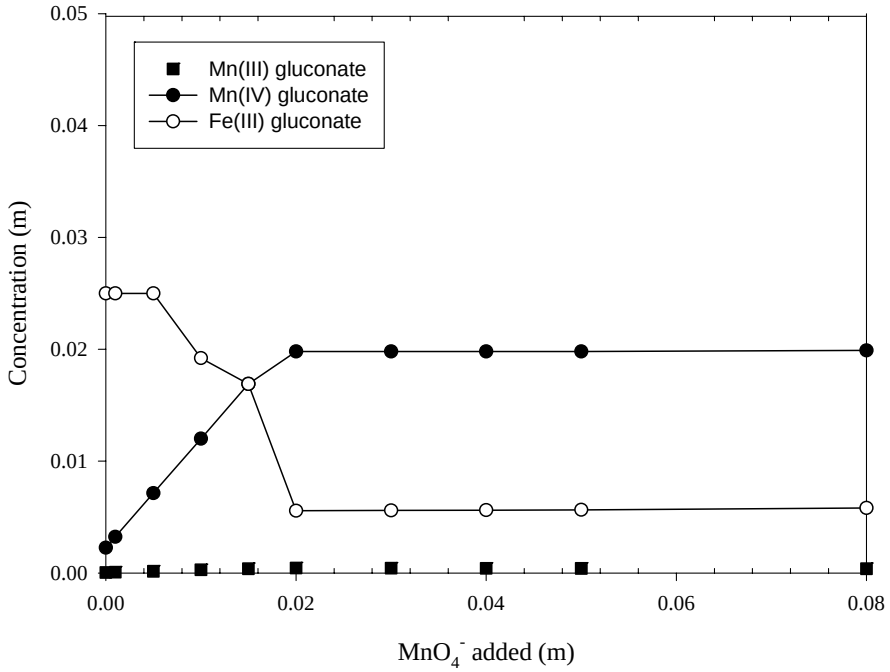

Figure 4.1. Gluconate-Containing Species Calculated to Form in AN-107 Feed Following Permanganate Additions

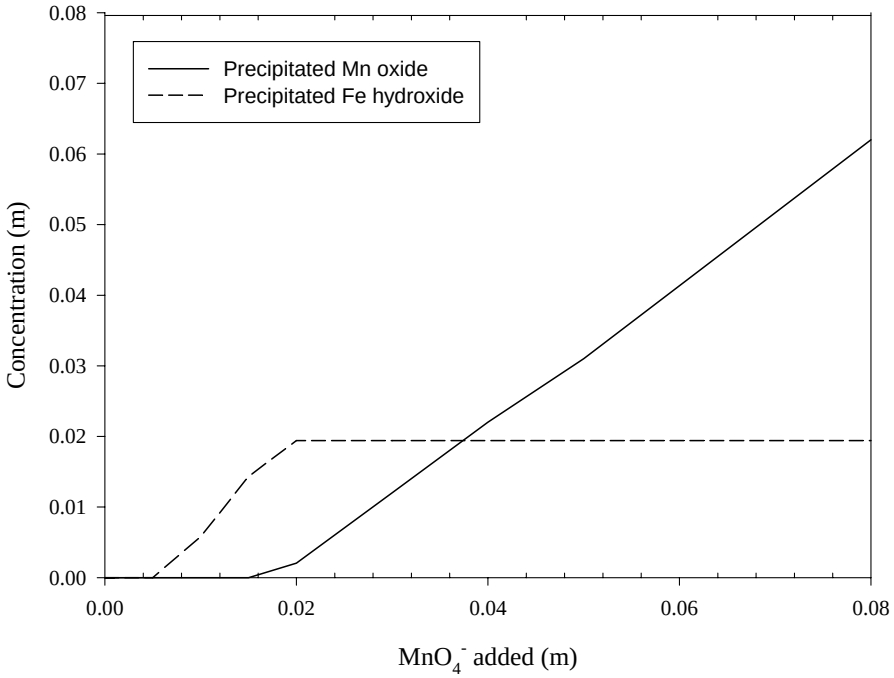

Figure 4.2. Calculated Iron Hydroxide and Manganese Oxide Formation in AN-107 Feed Following Permanganate Addition. The designation (m) in this case refers to moles of solid precipitated per kilogram of water in solution.

5.0 Conclusions and Recommendations

An extensive literature review and analysis of thermodynamic data for the modeling of Sr and Mn was conducted. New data were analyzed where literature data were not available or did not adequately match the conditions relevant to the Sr/TRU removal process. This work provided a better understanding of the Sr/TRU removal process. Conclusions from this work and recommendations to consider for plant operation are presented in this section.

Understanding Sr-EDTA complexation is extremely important for modeling the Sr/TRU removal process for Envelope C wastes. EDTA is in significant concentration and has the greatest impact on understanding Sr-90 removal. Sr-90 is removed from solution by isotopic dilution with added nonradioactive Sr and precipitation as $SrCO_3$. The $SrCO_3$ precipitation is strongly influenced by the composition of the waste, time, and temperature. The [Na] was found to have a large impact on the formation of the Sr-EDTA complex, as well as $[CO_3]$. The retrograde solubility behavior of $SrCO_3$ observed in actual waste tests is supported by the thermodynamic data presented in this study. The time to reach equilibrium for the Sr-EDTA mixtures was found to be quite long; generally more than a week was required.

The Sr-HETDA complexation is quite similar to EDTA, with a few exceptions. The [Na] effect is much less, and equilibration was faster. The results based on $[CO_3]$ and temperature were similar for both chelators. The modeling results support the mechanistic understanding of the Sr-90 removal process. The important factors for determining Sr-90 decontamination are the isotopic dilution ratio and the [Sr]. The isotopic dilution is quite rapid relative to $SrCO_3$ precipitation. The [Sr] is a function of waste composition and temperature. Higher carbonate concentration and temperature favor Sr-90 removal. In the treatment scheme, over 95% of the added Sr is precipitated from solution.

Gluconate forms quite strong complexes with Mn ions (IV, III, and II). Using available literature data to predict the thermodynamic stabilities of the various Mn-gluconate species, the Mn(IV) complex was shown to be the most stable. The stability of the Mn complex can be compared to the literature values reported for the Fe complex. Using these results, the Mn was shown to displace the Fe from the complex, precipitating all the complexed Fe. Unfortunately, the permanganate also oxidized a significant amount of the gluconate. The model could not account for this reaction. The ligand displacement reaction by added metal ions is consistent with the experimental results of Lilga et al. (2003) and Hallen et al. (2003), where Zr(IV) addition was found to remove TRU from solution. Accurate modeling of the permanganate treatment process would require extensive kinetic and thermodynamic data on the oxidation of organics by added permanganate. Such a database would require years of additional experimental work. However, the process works well and such an effort is not warranted for this project.

6.0 References

Anderegg, G. 1975. "Critical Survey of Stability Constants of EDTA Complexes." IUPAC Chemical Data Series, No. 14. Pergamon Press, New York.

Barney, G. S. 1996. *Solubilities of Significant Organic Compounds in HLW Tank Supernatant Solutions - FY 1996 Progress Report*. WHC-EP-0899-1, Westinghouse Hanford Company. Richland, WA.

Bhat, T. R., R. R. Das, and J. Shankar. 1967. "Complexes of Aluminum with Some Polyaminopolycarboxylic Acids." *Indian Journal of Chemistry* 5: 324-327.

Bodini, M. E., L. A. Willis, T. L. Riechel, and D. T. Sawyer. 1976. "Electrochemical and Spectroscopic Studies of Manganese (II), - (III), and - (IV) Gluconate Complexes 1. Formulas and Oxidation-Reduction Stoichiometry." *Inorganic Chemistry* 15(7):1538-1543.

Botts, J., A. Chashin, and H. L. Young. 1965. "Alkali Metal Binding by Ethylenediaminetetraacetate, Adenosine 5'-Triphosphate, and Pyrophosphate." *Biochemistry* 4:1788-1796.

Busenberg, E., and L. N. Plummer. 1984. "The Solubility of Strontianite ($SrCO_3$) in CO_2-H_2O Solutions Between 2 and 91°C, the Association Constants of $SrHCO_3^+$(aq) and $SrCO_3$(aq) Between 5 and 80°C, an Evaluation of the Thermodynamic Properties of Sr^{2+}(aq) and $SrCO_3$(cr) at 25°C and 1 atm Total Pressure." *Geochmica et Cosmochimica Acta* 48:2021-2035.

Carini, F. F., and A. E. Martell. 1954. "Thermodynamic Quantities Associated with the Interaction Between Ethylenediaminetetraacetate and Alkaline Earth Ions." *Journal of American Chemical Society* 76(8):2153-2157.

Chen, M., and R. S. Reid. 1993. "Solution Speciation in the Aqueous Na(I)-EDTA and K(I)-EDTA Systems." *Canadian Journal of Chemistry* 71:763-768.

Daniele, P. G., C. Rigano, and S. Sammartano. 1985. "Ionic Strength Dependence of Formation Constants. Alkali Metal Complexes of Ethylenediaminetetraacetate, Nitrilotriacetate, Diphosphate, and Tripolyphosphate in Aqueous Solution." *Analytical Chemistry* 57:2956-2960.

Felmy, A. R. 2000. *Thermodynamic Modeling of Sr/TRU Removal*. PNWD-3044, Rev. 0, Battelle, Pacific Northwest Division. Richland, WA.

Felmy, A. R., D. A. Dixon, J. R. Rustad, M. J. Mason, and L. M. Onishi. 1998. "The Hydrolysis and Carbonate Complexation of Strontium and Calcium in Aqueous Electrolytes: Use of Molecular Modeling Calculations in the Development of Aqueous Thermodynamic Models." *Journal of Chemical Thermodynamics* 30:1103-1120.

Felmy, A. R., and G. T. MacLean. 2001. *Development of an Enhanced Thermodynamic Database for the Pitzer Model in ESP: The Fluoride and Phosphate Components*. PNWD-3120, Battelle, Pacific Northwest Division, Richland, WA.

Felmy, A. R., and M. J. Mason. 1998. "The Displacement of Sr from Organic Chelates by Hydroxide, Carbonate, and Calcium in Concentrated Electrolytes." *Journal of Solution Chemistry* 27(5):435-454.

Felmy, A. R., and M. J. Mason. 2003. "An Aqueous Thermodynamic Model for the Complexation of Sodium and Strontium with Organic Chelators Valid to High Ionic Strength. I. N-(2-hydroxyethyl)ethylenedinitrilotriacetic acid (EDTA)." *Journal of Solution Chemistry* 32(4):283-300.

Felmy, A. R., M. J. Mason, and O. Qafoku. 2003. "An Aqueous Thermodynamic Model for the Complexation of Sodium and Strontium with Organic Chelators valid to High Ionic Strength. II. N-(2-hydroxyethyl)ethylenedinitrilotriacetic acid (HEDTA)." *Journal of Solution Chemistry* 32(4):301-318.

Felmy, A. R., D. Rai, J. A. Schramke, and J. L. Ryan. 1989. "The Solubility of Plutonium Hydroxide in Dilute-Solution and in High-Ionic-Strength Brines." *Radiochimica Acta* 48:29-35.

Felmy, A. R., J. R. Rustad, M. J. Mason, and R. de la Bretonne. 1994. *A Chemical Model for the Major Electrolyte Components of the Hanford Waste Tanks*. TWRS-PP-94-090, Westinghouse Hanford Co. Richland, WA.

Felmy, A. R., and J. H. Weare. 1986. "The Prediction of Borate Mineral Equilibria in Natural Waters: Application to Searles Lake, California." *Geochmica et Cosmochimica Acta* 50:2771-2783.

Hallen, R. T., J. G. H. Geeting, M. A. Lilga, and F. V. Hoopes. 2003. *Assessment of Sr/TRU Removal Mechanisms Using AN-102 and AN-107 Tank Waste Samples*. WTP-RPT-082, Battelle, Pacific Northwest Division (to be published).

Hallen, R. T., Geeting, J.G.H., Jackson, D. R., and D. R. Weier. 2002. *Combined Entrained Solids and Sr/TRU Removal from AN-102/C-104 Waste Blend.* PNWD-3264, Battelle, Pacific Northwest Division, Richland, WA.

Hallen, R. T., P. R. Bredt, K. P. Brooks, and L. K. Jagoda. 2000. *Combined Entrained Solids and Sr/TRU Removal from AN-107 Diluted Feed*. BNFL-RPT-027, Battelle, Pacific Northwest Division, Richland, WA.

Harvie, C. E., N. Moller, and J. H. Weare. 1984. "The Prediction of Mineral Solubilities in Natural Waters: The Na-K-Mg-Ca-H-Cl-SO_4-OH-HCO_3-CO_3-CO_2-H_2O System to High Ionic Strengths at 25°C." *Geochmica et Cosmochimica Acta* 48:723-751.

Hovey, J. K., L. G. Hepler, and P. R. Tremaine. 1988. "Thermodynamics of Aqueous EDTA Systems: Apparent and Partial Molar Heat Capacities and Volumes of Aqueous $EDTA^{4-}$, $HEDTA^{3-}$, H_2EDTA^{2-}, $NaEDTA^{3-}$, and $KEDTA^{3-}$ at 25°C. Relaxation Effects in Mixed Aqueous Electrolyte Solutions and Calculations of Temperature Dependent Equilibrium Constants." *Canadian Journal of Chemistry* 66:881-896.

James, T. L., and J. H. Noggle. 1969. "Sodium-23 Nuclear Magnetic Resonance Studies of Sodium Aminocarboxylic Acid Complexes." *Journal of American Chemical Society* 91(13):3424-3428.

Kolthoff, I. M., and J. J. Lingane. 1952. "Theoretical Principles Instrumentation and Technique. Polarography," Vol. 1. Interscience Publishers, New York - London.

Lilga, M. A., Hallen, R. T., K. M. Boettcher, T. R. Hart, and D. S. Muzatko. 2003. *Assessment of the Sr/TRU Removal Precipitation Reaction Mechanisms Using Waste Simulant Solutions*. PNWD-3263, Battelle, Pacific Northwest Division, Richland, WA.

Martell, A. E., and R. M. Smith. 1995. "Critically Selected Stability Constants of Metal Complexes Database," Version 2.0. NIST Standard Reference Data Program, Gaithersburg, MD.

Merciny, E., J. M. Gatez, and G. Duyckaerts. 1976. "Etude Thermodynamique De La Complexation Des Lanthanides Trivalents Avec L'Acide Hydroxylethylethylenediaminetriaacetique et D'Autres Acides Aminoacetiques II. Determination Par Potentiometrie Des Constantes D'Acidite De L'Acide Hydroxyethylenediaminetriacetique." *Analytica Chimica Acta* 86:247-254.

Mizera, J., A. H. Bond, G. R. Choppin, and R. C. Moore. 1999. "Dissociation Constants of Carboxylic Acids at High Ionic Strengths." *Actinide Speciation in High Ionic Strength Media: Experimental and Modeling Approaches to Predicting Actinide Speciation and Migration in the Subsurface*, eds., D. T. Reed, S. B. Clark, and L. Rao, pp. 113-124. Kluwer Academic/Plenum Publishers, New York,.

Nelson, F. 1955. "Anion-exchange Studies. XIV. The Alkali Metals of Ethylenediaaminetetraacetic Acid Solutions." *Journal of American Chemical Society* 77:813-814.

Oyama, N., T. Shirato, H. Matsuda, and H. Ohtaki. 1976. "A Potentiometric Study of Complex Formation of Cadminum (II) and Lead (II) Ions with N-(2-Hydroxyethyl)ethylenediamine-N,N',N'-triacetic Acid." *Bulletin of the Chemical Society of Japan* 49(11):3047-3052.

Pabalan, R. T., and K. S. Pitzer. 1987. "Thermodynamics of NaOH(aq) in Hydrothermal Solutions." *Geochmica et Cosmochimica Acta* 51:1093-1111.

Palaty, V. 1963. "Sodium Chelates of Ethylenediaaminetetraacetic Acid." *Canadian Journal of Chemistry* 41:18-21.

Peiper, J. C., and K. S. Pitzer. 1982. "Thermodynamics of the Aqueous Carbonate Solutions Including Sodium Carbonate, Bicarbonate, and Chloride." *Journal of Chemical Thermodynamics* 14:613-638.

Pitzer, K. S. 1973. "Thermodynamics of Electrolytes. I. Theoretical Basis and General Equations." *Journal of Physical Chemistry* 77:268-277.

Pitzer, K. S. 1991. *Activity Coefficients in Electrolyte Solutions*. CRC Press, Boca Raton, FL.

U.S. Department of Energy (DOE), Office of River Protection. 2000. *Contract Between DOE Office of River Protection and Bechtel National, Inc. for the Design, Construction, and Commissioning of the Hanford Tank Waste Treatment and Immobilization Plant (WTP).* Contract DE-AC27-01RV14136, Richland, WA.

Vasil'ev, V. P., and A. K. Belonogova. 1976. "Thermodynamic Characteristics of the Formation of the Ethylenediamine-tetra-acetato-complex of Sodium in Aqueous Solution." *Russian Journal of Inorganic Chemistry* 21(3):350-353.

Wright, D. L., J. H. Holloway, and C. N. Reilley. 1965. "Heats and Entropies of Formation of Metal Chelates of Polyamine and Polyaminocarboxylate Ligands." *Analytical Chemistry* 37(7):884-892.

Appendix

Calculation of Standard-State Equilibrium Constants from Half-Wave Potentials

This appendix presents an example calculation of the standard-state equilibrium constants from the experimental half-wave potentials. The example is for the Mn(IV)/Mn(III) reaction.

We begin with the half-cell reaction:

$$Mn(IV)(GH_3)_2(OH)_3^{3-} + e^- \Leftrightarrow Mn(III)(GH_3)_2OH^{2-} + 2OH^- \quad (1)$$

Now to obtain an overall thermodynamic reaction there must be a corresponding oxidation half-reaction occurring in the reference cell. In the actual reference cell this reaction is,

$$Ag + Cl^- (TMAC) \Leftrightarrow AgCl + e^- \quad (2)$$

Although, the TMAC concentration was not reported, Bodini et al. (1976) adjusted the TMAC concentration in the cell until a zero emf was obtained against the SCE. The SCE oxidation reaction is,

$$Hg + Cl^- (sat\ KCl) \Leftrightarrow \tfrac{1}{2}Hg_2Cl_2 + e^- \quad (3)$$

So in the case of the SCE reference electrode the overall cell reaction would be,

$$Mn(IV)(GH_3)_2(OH)_3^{3-} + Hg + Cl^-(sat\ KCl) \Leftrightarrow Mn(III)(GH_3)_2OH^{2-} + 2OH^- + \tfrac{1}{2}Hg_2Cl_2 \quad (4)$$

The potential of this cell is given by

$$E = E^0 - RT/F\ lnQ + E_j \quad (5)$$

where E^0 is the standard emf of the cell, Q is the activity product for reaction (4), and E_j is the liquid junction potential.

Now to determine equilibrium constants we must find E^0 since this is directly related to the thermodynamics of reaction, i.e.,

$$\Delta G^0_r = -nFE^0 = -RTlnK^0$$

where ΔG^0_r is the standard free energy of reaction and K^0 is the standard-state equilibrium constant. So the problem involves using the measured half-wave potential and determining lnQ and E_j to obtain E^0.

In the case of the SCE, liquid junction potentials are usually quite small (on the order of millivolts), owing to the high concentration of KCl diffusing through the liquid junction, so to a first approximation this term can be neglected. With this assumption the problem reduces to calculation of Q, which is given by,

$$\ln Q = a\{Mn(III)(GH_3)_2OH^{2-}\} x\ a^2\{OH^-\}/(a\{Cl^- \text{ in KCl}\} x\ a\{Mn(IV)(GH_3)_2(OH)_3^{3-}\}$$

where a represents activity. In the case of the half-wave potentials, the concentrations of the oxidized and reduced species are equal; the total concentration of Mn in solution is reported (0.001m); the concentration of hydroxide is known (0.3m); and the concentration of chloride in equilibrium with KCl is also known (4.854m). Thus, if activity coefficients are neglected the expression for lnQ is,

$$\ln Q = \ln[(0.0005m)(0.3m)2/(0.0005m)(4.854)] = -3.988$$

or

$$RT/F\ \ln Q = -0.102V$$

if the Pitzer thermodynamic model is used to calculate the activity coefficients using the known coefficients for chloride and hydroxide (Harvie et al. 1984) combined with charge analogs for the Mn complexes based on an analogy with EDTA complexes of the same charge (coefficients from Mizera et al. 1999). Then, the value of RT/F lnQ = -0.0625V. Combining this estimate with the neglect of the liquid junction potential yields,

$$E^0 = -0.33V \text{ versus SCE.}$$

Reaction (4) can also be rewritten versus the normal hydrogen electrode (NHE) via the reaction,

$$\tfrac{1}{2}H_2(g) + OH^- + \tfrac{1}{2}Hg_2Cl_2 \Leftrightarrow Hg + Cl^-(KCl) + H_2O,\ E^0 = 1.095V$$

yielding,

$$Mn(IV)(GH_3)_2(OH)_3^{3-} + \tfrac{1}{2}H_2(g) \Leftrightarrow Mn(III)(GH_3)_2OH^{2-} + OH^- + H_2O\ \ E^0 = 0.765 \qquad (6)$$

This is the value shown in the last column in Table 4.1. The values for E^0(NHE) for the other reactions in Table 4.1 were calculated in a similar manner. These values were then combined with the Mn(0) to Mn^{2+} oxidation reaction, i.e.,

$$Mn(0) + 2H^+ \Leftrightarrow Mn^{2+} + H_2(g),\ \text{Log K} = 39.96$$

calculated from the thermodynamic data in Wagman et al. (1982) to obtain the Log K values shown in Table 4.2.

References

Bodini, M. E., L. A. Willis, T. L. Riechel, and D. T. Sawyer. 1976. "Electrochemical and Spectroscopic Studies of Manganese (II), - (III), and - (IV) Gluconate Complexes 1. Formulas and Oxidation-Reduction Stoichiometry." *Inorganic Chemistry* 15(7):1538-1543.

Harvie, C. E., N. Moller, and J. H. Weare. 1984. "The Prediction of Mineral Solubilities in Natural Waters: The Na-K-Mg-Ca-H-Cl-SO_4-OH-HCO_3-CO_3-CO_2-H_2O System to High Ionic Strengths at 25°C." *Geochmica et Cosmochimica Acta* 48:723-751.

Mizera, J., A. H. Bond, G. R. Choppin, and R. C. Moore. 1999. "Dissociation Constants of Carboxylic Acids at High Ionic Strengths." *Actinide Speciation in High Ionic Strength Media: Experimental and Modeling Approaches to Predicting Actinide Speciation and Migration in the Subsurface*, eds., D. T. Reed, S. B. Clark, and L. Rao, pp. 113-124. Kluwer Academic/Plenum Publishers, New York,.

Wagman, D. D., W. H. Evans, V. B. Parker, R. H. Schumm, I. Halow, S. M. Bailey, K. L. Churney, and R. L. Nuttall. 1982. "The NBS Tables of Chemical Thermodynamic Properties. Selected Values for Inorganic and C1 and C2 Organic Substances in SI Units." *J. of Phys. Chem. Ref. Data*, Vol. 2 Supplement 2. American Chemical Society and the American Institute for Physics, New York.

Distribution

No. of Copies

OFFSITE

2 **Savannah River Technology Center**
Jim Marra
Savannah River Technology Center
Building 773-43A
P.O. Box 616, Road 1
Aiken, South Carolina 29808

Harold Sturm
Savannah River Technology Center
Building 773-A
P.O. Box 616, Road 1
Aiken, SC 29808

No. of Copies

ONSITE

8 **Battelle Pacific Northwest Division**

A. R. Felmy (2)	K8-96
D. E. Kurath	P7-28
O. Qafoku	K8-96
Project File (2)	P7-28
Information Release (2)	K1-06

6 **Bechtel National, Inc.**

W. L. Graves	H4-02
H. R. Hazen	H4-02
R. A. Peterson	H4-02
P. S. Townson	H4-02
W. L. Tamosaitis	H4-02
WTP PDC Submittal Coordinator	H4-02

2 **CHG2M Hill Hanford Group, Inc.**

D. A. Reynolds	S7-90
K. Gasper	H6-03

1 **Fluor Federal Services**

G. T. MacLean	E6-40

1 **Fluor Hanford**

D. L. Herting	T6-07

1 **Numatec Hanford Corporation**

J. L. Jewett	G3-43